CHESTER

Compressed Heat Energy Storage for Energy from Renewable sources

Operation modes and control strategies to be implemented at CHEST laboratory prototype

PROJECT	**CHESTER**
PROJECT NO.	**764042**
DELIVERABLE NO.	**D4.4**
DOCUMENT VERSION	**6**
DOCUMENT PREPARATION DATE	**16-11-2020**
RESPONSIBILE PARTNER	**AIGUASOL**
DISSEMINATION LEVEL	**Public**

Type of Deliverable		
R	Document, Report	**x**
DEM	Demonstrator, pilot, prototype	
DEC	Websites, patent fillings, videos, etc.	
OTHER		
ETHICS	Ethics requirements	
ORDP	Open Research Data Pilot	

This project has received funding from the European Union's Horizon 2020 research and innovation programme under grant agreement No. 764042.

EC Grant Agreement	No.764042
Project Acronym	CHESTER
Project Title	Compressed Heat Energy Storage for Energy from Renewable sources
Programme	HORIZON 2020
Start Date of Project	01-04-2018
Duration	48 Months

Financial/Administrative Coordinator	
Project Coordinator Organization Name	TECNALIA
Address	Parque Tecnológico de Bizkaia C/Astondo, Edificio 700 (Spain)
Phone Numbers	+34 946 430 850
E-mail Address	nora.fernandez@tecnalia.com
Project web-site	www.chester-project.eu

Version Management			
Filename		D4.4: Operation modes and control strategies to be implemented at CHEST system	
Author(s)		A. Carrera/S.Stark	
Reviewed by		H.Jockenhoefer/M. Johnson	
Approved by		N. Fernandez	
Revision No.	**Date**	**Author**	**Modification description**
RV 1	24-09-2020	A:Carrera/S.Stark	First version of the document
RV 2	1-10-2020	S.Stark	Upgrade on section 3
RV 3	6-10-2020	A.Carrera	Upgrade Section 1, section 5 and formatting
RV 4	28-10-2020	A.Carrera	Nomenclature review to match with WP6
RV 5	9-11-2020	H.Jockenhoefer/M. Johnson	Document review
RV6	12-11-2020	G. Barroso	Grammar and spelling review
RV 7	13-11-2020	S. Stark	Review comments included
RV 8	16-11-2020	A.Carrera	Review comments included

Contents

List of Figures

List of Tables

Glossary, abbreviations and acronyms

CF	Capacity Factor
CHEST	Compressed Heat Energy Storage
CHP	Combined Heat and Power system
COP	Coefficient of Performance
DH	District Heating network
DSO	Distribution System Operator
GWP	Global Warming Potential
HX	Heat eXchanger
HP	Heat Pump
HTTES	High Temperature Thermal Energy Storage
NBP	Normal Boiling Point
NEMO	Nominated Electricity Market Operator
ODP	Ozone Depletion Potential
ORC	Organic Rankine Cycle
P2P	Power to Power ratio
PCM	Phase Change Material
PHS	Pumped Hydro Storage
PV	Photovoltaics
SoC	State of Charge

1. Introduction

1.1. Executive Summary

This document describes the analysis of the control strategies for the CHEST system connected to the energy networks. To do this, it became necessary to analyze different combinations of the pair PCM/refrigerant to find the most appropriate combination that best fit to the specific heat sink and source temperatures of the two case studies analyzed in WP4. This yielded results that allow to a better understanding of the incidence of the refrigerant and PCM properties on the overall performance of the system when delivering the specific grid services foreseen at each case study.

This is part of the WP4 workflow, that aims on the last term to optimize the integration of the CHEST systems on the energy system with the will to maximize the potential of the technology. The analysis here is done based on simulation results from a TRNSYS [1] software model developed in T4.2. This model is focused on characterizing the integration of the CHEST system into energy grids, and the boundary conditions like energy demands, energy prices, meteorological data and waste heat availability are based on the monitoring data from the case studies gathered within T4.1.

The optimization of the system required to this project task started with the characterization of a wide set of potential PCM and refrigerants that could improve the CHEST performance. The selection of materials has strong implications on the temperature level of the heat pump and the Organic Rankine Cycle, hence also, on the system performance. Due to this, it was deemed necessary to select appropriate combinations of materials for each case study. This first set of simulations covered 42 potential combinations, and the section 2 of this deliverable describes the criteria for selecting the materials, as well as the results of the literature analysis on the topic. The selection relied also on the expert project partners on these specific fields.

The results of the simulations showed that, as suspected, the specific characteristics of each of the case studies could fit better to different PCM and refrigerant combinations. The analysis in section 3 also shows that even slight changes on the Ispaster case study can make a difference in the optimal material selection. Beyond this specific objective for the project, a set of trends of the system performance dependence upon physical characteristics of the materials was identified. For instance, the growing economic return with increasing melting temperature of the PCM or the dependence of the system heat requirement with the refrigerant properties are examples of this trends that can be further considered in the CHEST development. This trend as well as other simulation results are presented in section 3. One of the important conclusions of the analysis presented there is the impact of the materials on the sizing of the system components, that may reduce the investment on the CHEST system substantially.

The second set of simulations was done with the preselected refrigerant and PCM materials combination selected in the previous run of simulations. In this stage, the aim was to compare how the different control strategies for the CHEST system can affect the performance when the system is incorporated into the electrical grid. Up to 16 different temperature levels scenarios for the HP evaporator and the ORC condenser were simulated and the analysis is presented in section 4. The main outcome of this set of simulations is the evidence that the CHEST electricity services are opposed to the thermal energy services, since as the results show, the higher the electricity charged and discharged by the CHEST system, the higher is the heat requirement by the system. This has strong implications on the business model of the CHEST system and shall be taken into account in the future.

1.2. Purpose and Scope

The purpose of this deliverable is to summarize the results regarding the control strategies optimisation of the CHEST system. Due to the fact that those control strategies may vary significantly depending on the PCM and refrigerant used to design the system, an initial study was done to assess the performance of different potential combinations of materials. This is a preliminary and necessary step towards the optimisation under the energy market conditions, which led to relevant conclusions that are also presented here.

1.3. Methodology

The work described in this document is, as stated in the project workplan, based on the TRNSYS model of the CHEST system developed in Task 4.2. The aim of the model is to analyze the integration of the CHEST system into the energy networks (electrical grid as well as DH networks). First, a literature survey was done to screen a set of pairs of refrigerant and PCM materials that could be used in the characteristic temperature range of the CHEST system. After gathering the necessary thermophysical properties of the selected materials, they were included in the TRNSYS model of T4.2 to compare their performance and select the most appropriate combination for each case study. Finally, with the selected materials fixed, a new set of simulations was done to assess quantitatively the performance of the system for the case studies for the system operation modes.

1.4. Structure of the document

As stated in the project workplan, the work described in this document is based on the TRNSYS model of the CHEST system developed in Task 4.2. The aim of the model is analysing the integration of the CHEST system into the energy networks (electrical grid as well as DH networks). First, a literature survey was done to identify a set of pairs of refrigerant and PCM materials that could be used in the characteristic temperature range of the CHEST system. After gathering the necessary thermophysical properties of the selected materials, they were included in the TRNSYS model of T4.2 to compare their performance and select the most appropriate combination for each case study. Finally, with the selected materials fixed, a new set of simulations was done to assess quantitatively the performance of the system for the case studies for the system operation modes.

1.5. Relations with other deliverables

This work is interrelated with several deliverables on the project; first, it relies on the findings of WP2 and the model developed by Aiguasol in T4.2 to develop the conclusions. The results will be used in the future work to be carried out in T4.4, the SEMS development, that will be characterized by the findings included in this document. Also, it is foreseen to feed the WP5, since the control strategies described will be implemented in the testing and, moreover, it has implications to WP6 due to the fact that the results will be used to improve the calculations of the T6.5, the CHEST webtool. Finally, the conclusions drawn here have implications on the exploitation potential of the CHEST system, so they can be eventually used by the WP6 as a whole to improve the exploitation strategies of the CHEST system.

2. Screening of PCMs and refrigerants for the CHEST system

2.1. Introduction

The need of a closer look on the refrigerant selection for the CHEST system is based on the diversity of situations where the CHEST concept can be applied. The case studies analysis shows a wide range of potential source (waste heat, solar thermal energy, biomass) and sink temperatures (DH network or ambient temperature) for the CHEST system, which as shown in D2.2, have a fundamental impact on the overall system performance since the HP evaporator temperature and the ORC condensing temperature are directly related to these values.

Also, there is a need to look for alternative PCMs, mainly because of two reasons. First, if the abovementioned required temperature difference of 20 K is considered and the melting temperature is kept at 133 °C, this means that the evaporation temperature level of the ORC will account for only 113 °C. This will result in a relatively low temperature difference between evaporation and condensation temperature level and therefore a relatively low efficiency of the ORC. Hence, suitable PCMs with higher melting temperatures should be identified. Second, as was mentioned above, the low thermal conductivity is the key problem here for the limitation of the heat transfer inside the PCM storage. Therefore, PCMs with higher thermal conductivities should be identified. A higher thermal conductivity would also lower the required temperature difference between the working fluid and the PCM.

This would actually be beneficial, because, such a high temperature difference of 20 K is disadvantageous for the overall efficiency of the CHEST process, as has been shown by Jockenhöfer et al. [2]. For thermodynamic reasons, a low temperature difference between the two media in a heat exchanger is favorable.

Furthermore, it must be considered that an increase of the melting temperature of the PCM not only leads to a higher ORC efficiency, but also to a lower COP of the heat pump. So, the melting temperature of the PCM should not be too high, also for practical reasons: As has been shown by Arpagaus et al. [3], currently market-available heat pumps allow for a maximum condensation temperature of only about 165 °C. Maybe, there will be future developments here to reach even higher condensation temperatures, but it should be considered, that also the complexity of the whole process might increase, for instance through the need of a two-stage compression.

In the analysis presented in this document, the focus was laid on the look for PCMs with a melting temperature in the range 140 - 180 °C and for refrigerants with a critical temperature of at least 160 °C. After the overview on the analysis of PCMs (Section 2.2) and refrigerants (Section 2.3), a final conclusion is drawn and a suggestion is given on which PCM-refrigerant combinations could be subject to comparative TRNSYS simulations in T4.4.

2.2. PCM selection

2.2.1. Properties for PCM selection

Table 1 shows an overview of relevant PCM selection properties and their respective importance. The section below the table discusses this briefly.

Table 1: PCM selection properties.

Property	Target	Importance
Phase change temperature [°C]	in the range of ca. 140 - 180 °C, see Chapter 1	decisive for the work considered in T4.4
Thermal conductivity [mW/(m·K)]	as high as possible	very high
Phase change enthalpy [kJ/kg]	as high as possible	high
Density [kg/m³]	as high as possible	medium
Specific heat capacity [J/(kg·K)]	as high as possible	medium
Dynamic viscosity [µPa·s]	as low as possible	low
Volume change at phase change [%]	as low as possible	low
Thermal expansion coefficient [1/K]	as low as possible	low
Corrosion	as low as possible	low (at the moment)
Cyclic stability	as high as possible	low (at the moment)
Toxicity	as low as possible	low (at the moment)
Maximum operating temperature	as high as possible	low (at the moment)
Price [€/kg]	as low as possible	low (at the moment)

As explained in the introduction, the task here is to look for PCMs which are suitable for the CHEST application considered in this project, i.e. most importantly, the **phase change temperature** has to be in the proper range of 140 - 180 °C. A PCM with lower phase change temperature does not make sense for this CHEST application, because the abovementioned necessary temperature difference between PCM and working fluid of 20 K results in an evaporation temperature of the working fluid in the ORC circuit of about 90 °C. This will result in a low temperature difference between ORC evaporation and condensation temperature and therefore in low ORC efficiencies. On the other hand, phase change temperatures above 180 °C will result in low COPs of the heat pump. Furthermore, the heat pump process is likely to get more complicated at higher temperatures.

Beside the phase change temperature, the **thermal conductivity** is the most important property to be considered here. As was pointed out in D4.2, the generally low thermal conductivity of PCMs means a high thermal resistance to the transfer of heat from the HX pipes inside the HTTES into the PCM interior. Many research groups are working on the PCMs thermal conductivity in order to improve load management in practical applications. The most common approaches include the use of extended heat exchange surfaces, mixing of the PCM material with metal nanoparticles or other conductive materials or the use of different

Further properties with a lower impact on the heat transfer inside the PCM storage are the **specific heat capacity**, the **viscosity** and the **thermal expansion coefficient**. All three are involved in the PCM convective heat transfer (see D4.2 for details on how this is calculated) . Moreover, the specific heat capacity has also influence on some sensible heat (stored in overheated PCM), which is however almost negligible compared to the latent heat in small temperature ranges. As regards to heat transfer and sensible heat, the specific heat capacity should be as high as possible.

A more important property is the **phase change enthalpy**. It should be as high as possible to allow for a compact PCM storage. For the same reason, the **density** of the PCM should be high.

During phase change and heating/cooling, the density of a material changes. The resulting change of volume should be as low as possible as it must be compensated for by providing the respective additional space. Therefore, **volume change at phase change** and the **thermal expansion coefficient** should be low. However, together with the viscosity, these properties are assessed as of lower importance for the selection of the PCM here.

The properties corrosion, cyclic stability, toxicity and maximum operating temperatures are important for the practical use of the PCM in a storage system. However, for the analysis of the potential of different PCM/refrigerant combinations in T4.4, it is assessed to be of minor importance. Furthermore, it must be said that very little information is available concerning these properties at the moment.

The **price** of the PCM is certainly always an important criterion in the selection of the PCM. However, for this analysis, it is seen as of minor importance at the current state of PCM storage development for a CHEST system.

The properties thermal conductivity, density, specific heat capacity, (viscosity) and the thermal expansion coefficient have to be considered in both the solid and the liquid states.

2.2.2. Result of the literature analysis

For the analysis carried out in this document, mainly the sources [4] [5] [6] [7] and [8] were used. As can be seen from these sources, there are several groups of PCMs like organic materials (e.g. paraffins), inorganic materials (e.g. salt hydrates), eutectic mixtures and solid-solid PCMs. The advantages and disadvantages are not discussed here, but can be found in the aforementioned sources.

As a result of the analysis, Table 2 lists those PCMs that satisfy the following criteria:

- suitable phase change temperature, i.e. 140 - 180 °C
- reported thermal conductivity of at least 500 mW/(m·K)

The reason for this latter criterion is that it is not really reasonable to consider PCMs with a lower thermal conductivity, because this would limit the heat transfer in the PCM storage too strongly. Table 2 lists the properties of the initially considered PCM KNO_3-$LiNO_3$ for comparison. Values for the viscosity, the volume change and the thermal expansion coefficient were not found and were therefore omitted.

As can be seen from the table, these are in principle all eutectic mixtures. As regards to the phase change temperature, also several organic and inorganic materials are also interesting. However, their thermal conductivity is rarely reported in the sources or it is rather low, as for d-Mannitol with only 190 and 110 mW/(m·K) in solid and liquid state [8],respectively. Therefore, no such material was included in the table here.

Table 2: Main properties of relevant PCMs found in literature.

PCM	Type	Phase change tempera-ture [°C]	Thermal conductivity (solid) [mW/(m·K)]	Thermal conductivity (liquid) [mW/(m·K)]	Phase change enthalpy [kJ/kg]	Density (solid) [kg/m³]	Specific heat capacity (solid) [J/(kg·K)]	Specific heat capacity (liquid) [J/(kg·K)]	Price [€/kg]
$LiNO_3$-$NaNO_3$-KNO_3	eutectic	123 [4]	790 [8]	530 [8]	140 [8]	2068 [8]	1170 [8]	1440 [8]	1.14 [8]
KNO_3-$LiNO_3$	eutectic	133 [9]	960 [8]	520 [8]	170 [9] 150 [8]	2018 [8]	1170 [8]	1350 [8]	1.28 [8]
KNO_3-$NaNO_3$-$NaNO_2$	eutectic	142 [4]	720 [8]	570 [8]	80 [9] 110 [8]	2006 [8]	1170 [8]	1730 [8]	0.29 [8]
KNO_2-$NaNO_3$	eutectic	149 [4]	580 [8]	520 [8]	124 [8]	2080 [8]	1050 [8]	1630 [8]	0.57 [8]
$LiNO_3$-$NaNO_2$	eutectic	156 [4]	1120 [8]	660 [8]	233 [8]	2296 [8]	1570 [8]	1910 [8]	1.98 [8]
$LiNO_3$-$NaNO_3$-KCl	eutectic	160 [4]	880 [8]	590 [8]	266 [8]	2297 [8]	1320 [8]	1690 [8]	1.48 [8]
HCOONa-HCOOK	eutectic	176 [4]	630 [8]	430 [8]	175 [8]	1913 [8]	1150 [8]	930 [8]	0.26 [8]
$LiNO_3$-$NaNO_3$	eutectic	194 [4]	880 [8]	590 [8]	262 [8]	2317 [8]	1350 [8]	1720 [8]	1.58 [8]

In Table 2, the values were highlighted as regards to their level compared to the currently considered KNO_3-$LiNO_3$: light green (in the same range or slightly better), dark green (considerably better), yellow (worse) and orange (considerably worse). The two materials $LiNO_3$-$NaNO_2$ and $LiNO_3$- $NaNO_3$ -KCl show the best accordance with the required properties with phase change temperatures of 156 and 160 °C, respectively. They only drawback with these materials is the high price, which is however now considered as of minor importance.

All other materials show lower thermal conductivities compared to the currently considered PCM KNO_3-$LiNO_3$ in solid state. However, their thermal conductivity in liquid state is mostly slightly higher, except for HCOONa-HCOOK.

2.3. Refrigerant selection

2.3.1. Properties for refrigerant selection

Table 3 shows an overview of relevant refrigerant selection properties and their respective importance. The section below the table discusses this briefly.

Table 3: Refrigerant selection properties.

Property	Target	Importance
Critical temperature [°C]	≥ 160 °C, see Chapter 1	decisive for the work considered in T4.4
Shape of saturated vapor line	isentropic or almost isentropic	very high
Ozone depletion potential ODP [-]	must be zero	very high
Normal boiling point NBP [°C]	as low as possible	high
Global warming potential GWP [-]	as low as possible	high
Flammability	preferably low or non-flammable	high
Toxicity	preferably low or non-toxic	medium
Critical pressure [bar]	preferably low	medium
CoolProp availability	preferably yes	low
Specific volume at lower temperature level [m³/kg]	as low as possible	low
Thermal conductivity [mW/(m·K)]	as high as possible	low
Specific heat capacity [J/(kg·K)]	as high as possible	low
Dynamic viscosity [µPa·s]	preferably low	low
Price [€/kg]	as low as possible	low (at the moment)

As was said in the introduction, a proper heat transfer requires a certain temperature difference between the refrigerant and the PCM. This means that the **critical temperature** of the fluid has to be at least this temperature difference higher than the phase change temperature of the PCM, preferably a bit higher in order not to operate at the critical point. Given the minimum phase change temperature of 140 °C considered here, only refrigerants with a critical temperature of at least 160 °C are considered in the following.

The **shape of the saturated vapor line** is very decisive for the design of the HP and ORC process. As has been shown by [2] and [10], the shape should be isentropic or close to isentropic in the relevant temperature range. Otherwise, the process might become more complex, for instance due to the need of further heat exchangers.

Concerning environmental impact, the ozone depletion potential (**ODP**) is of most importance. This must be zero; otherwise, such a refrigerant is not sustainable and therefore will be phased out shortly. **GWP** is also important, but does not need to be zero. However, it should be as low as possible, preferably < 10 [10] .

NBP is important, because the pressure at the lower temperature level of the process (HP evaporation temperature level, ORC condensation temperature level) should not be below 1 bar. Otherwise, there is the risk of air suction into the system. This means that when NBP is for instance 60 °C, then the heat source for the HP process must be at least that high and ORC condensation cannot be done at temperatures below that in order to avoid refrigerant pressures below 1 bar. So, in order not to limit the HP evaporation and ORC condensation temperatures, NBP should be preferably low, let´s say < 60 °C.

Flammability and **toxicity** are quite important for the selection of a refrigerant, although not considered as a “K.O.-criterion” here, also because the currently considered refrigerant butene shows a high flammability.

The **critical pressure** should not be too high (preferably < 30 bar [28]), because equipment costs increase with increasing pressure.

The **CoolProp availability** is not a real fluid property, but it is considered here because of the intended TRNSYS simulations in Task 4.4. When the fluid is available in CoolProp, it can be easily integrated into the current TRNSYS model, which was developed in T4.2.

The **specific volume at lower temperature level**, i.e. at HP evaporation temperature level and ORC condensation temperature level, should be preferably low, i.e. the density should be high in order to keep components small and therefore cheap.

The **thermal conductivity** and the **specific heat capacity** are two properties that influence the heat transfer between fluid and PCM as has been shown in D4.2. They should be as high as possible to allow for a good heat transfer.

The **viscosity** has a minor influence also in heat transfer, but is more important for the operation of the compressor and expander, see D3.1.

Finally, the **price**, as was accordingly stated above for the PCM selection, is definitely an important issue, but in this analysis here and with regard to the actual status of the research project seen as of minor importance.

2.3.2. Result of the literature analysis

For the analysis carried out here, the sources [2], [3], [11] and [11] as well as the refrigerant data available in the software EES were used. Aside from these sources, other online available sources like safety data sheet were used). Table 4 shows the refrigerants found in the abovementioned sources, which satisfy the following criteria:

- critical temperature of at least 160 °C
- shape of saturated vapor line close to isentropic
- ODP (close to) zero
- NBP < 60 °C

The properties of the currently considered refrigerant butene (Isobutene) are also listed for comparison in Table 4.

Table 4: Refrigerant list and their properties

Name	Tcrit [K]	Pcrit [kPa]	RhoCrit [kg/m3]	NBP (K)	Shape of saturated vapor line	Flammability	Toxicity
Acetone	508.1	4700	272.98	329.2	Wet	High (H225)	H319, H336
Methanol	512.5	8215.8	273	337.7	Wet	High (H225)	H301, H311, H331 H370
Ethanol	514.7	6268	273.2	351.6	Wet	High (H225)	H319
Benzene	562	4894	304.8	353.2	Isentropic	High (H225)	H315, H361, H340, H350, H372, H304
Dimethyl carbonate	557	4908.8	360.3	363.2	Isentropic	High (H225)	-
Toluene	591.7	4126	292	383.7	Isentropic	High (H225)	H315, H319, H336, H373, H304
R1233zd (E)	439.6	3623.6	480.2	291.4	Isentropic	No	-
R1234ze (Z)	423.2	3530.6	470	282.9	Isentropic	No	-
Isobutene	419.2	4005.1	237.9	266.8	Dry	Very high (H220)	-
R601	469.7	3367.5	232	309.2	Dry	High (H225)	H336, H304
Cyclopentane	511.7	4571.2	267.9	322.4	Dry	High (H225)	-
Isohexane	497.7	3040	234	333.3	Dry	High (H225)	H304, H315, H336

The overview of properties in Table 4 shows that there is no fluid, which completely fits the requirements mentioned in Chapter 3.1 on the fluid selection criteria.

Moreover, there is the problem of high or very high flammability. If this can be handled, then the two pentanes, n-pentane and iso-pentane are the favorable fluids. Cyclopentane has a higher critical temperature, but on the other hand also a higher NBP of 49 °C. However, at least for the heat pump side, this is acceptable. Compared to the pentanes, acetone has an even higher NBP and also a relatively high critical pressure.

2.4. Refrigerant/PCM combinations

Beyond the specific individual characteristics of each PCM and refrigerant identified, not all the potential combinations among the materials listed in sections 2.2 and 2.3 are advisable or even feasible. So, a second step in the analysis is defining the potential combinations that will be included in the simulation work. To do so, two conditions are considered:

- There should be at least 20 K difference between the PCM melting temperature and the refrigerant critical temperature. As previously explained, this ensure that the system can be safely controlled.
- A maximum of 60 K temperature lift for the HP is allowed. The reason is that the HP COP diminishes as the required temperature lift increases, and 60 K is considered as a high limit based on the operational experience of high temperature heat pumps [3]

The second condition is equivalent to say that the difference between the heat pump evaporator temperature and the PCM melting temperature should never be bigger than 60 K. Hence, these conditions establish a different set of combinations for each case study, since the evaporator temperature is set by very different heat sources: industrial waste heat in the case of Aalborg, that has a very high temperature, while in Ispaster the heat source comes from a solar thermal field, that has a decreasing efficiency as working temperature increases. In the case of Ispaster, the working temperature is assumed to be 60° C which is a good compromise between temperature and efficiency for a solar thermal system. With this, the simulation sample, in table format, is defined as specified in the following tables. Table 4 includes the simulation sample for Aalborg, while the Table 5 sets the simulation scenarios for Ispaster.

Table 5: Simulation scenarios for the Aalborg case study.

Scenario	Refrigerant	PCM	HP evaporation temperature [°C]	ORC condensation temperature [°C]	PCM melting temperature [°C]
1	Acetone	$LiNO_3$-$NaNO_3$-KCl	100	55	160
2	Acetone	HCOONa-HCOOK	116	55	176
3	Acetone	$LiNO_3$-$NaNO_3$	134	55	194
4	Methanol	$LiNO_3$-$NaNO_3$-KCl	100	35	160
5	Methanol	HCOONa-HCOOK	116	35	176

6	Methanol	$LiNO_3$-$NaNO_3$	134	35	194
7	Ethanol	$LiNO_3$-$NaNO_3$-KCl	100	55	160
8	Ethanol	HCOONa-HCOOK	116	55	176
9	Ethanol	$LiNO_3$-$NaNO_3$	134	55	194
10	Benzene	$LiNO_3$-$NaNO_3$-KCl	100	55	160
11	Benzene	HCOONa-HCOOK	116	55	176
12	Benzene	$LiNO_3$-$NaNO_3$	134	55	194
13	Dimethyl carbonate	$LiNO_3$-$NaNO_3$-KCl	100	55	160
14	Dimethyl carbonate	HCOONa-HCOOK	116	55	176
15	Dimethyl carbonate	$LiNO_3$-$NaNO_3$	134	55	194
16	Toluene	$LiNO_3$-$NaNO_3$-KCl	100	55	160
17	Toluene	HCOONa-HCOOK	116	55	176
18	Toluene	$LiNO_3$-$NaNO_3$	134	55	194
19	R1233zd (E)	$LiNO_3$-$NaNO_3$-KNO_3	63	55	123
20	R1233zd (E)	$LiNO_3$-KNO_3	73	55	133
21	R1233zd (E)	KNO_3-$NaNO_3$-$NaNO_2$	82	55	142
22	R1234ze (Z)	$LiNO_3$-$NaNO_3$-KNO_3	63	55	123
23	Isobutene	$LiNO_3$-$NaNO_3$-KNO_3	63	55	123
24	R601	KNO_2-$NaNO_3$	89	35	149
25	R601	$LiNO_3$-$NaNO_2$	96	35	156
26	R601	$LiNO_3$-$NaNO_3$-KCl	100	35	160
27	Cyclopentane	$LiNO_3$-$NaNO_3$-KCl	100	35	160
28	Cyclopentane	HCOONa-HCOOK	116	35	176
29	Cyclopentane	$LiNO_3$-$NaNO_3$	134	35	194
30	Isohexane	$LiNO_3$-$NaNO_3$-KCl	100	35	160

31	Isohexane	HCOONa-HCOOK	116	35	176
32	Isohexane	$LiNO_3$-$NaNO_3$	134	35	194

Table 6: Simulation scenarios for the Ispaster case study.

Scenario	Refrigerant	PCM	PCM melting temperature [°C]	HP evaporation temperature [°C]	ORC condensation temperature [°C]
1	R1233zd(E)	$LiNO_3$-$NaNO_3$-KNO_3	123	63	70
2	R1233zd(E)	$LiNO_3$-KNO_3	133	73	70
3	R1233zd(E)	KNO_3-$NaNO_3$-$NaNO_2$	142	82	45
4	R1233zd(E)	KNO_3-$NaNO_3$-$NaNO_2$	142	82	70
5	Isobutene	$LiNO_3$-$NaNO_3$-KNO_3	123	63	55
6	Isobutene	$LiNO_3$-$NaNO_3$-KNO_3	123	63	70
7	R601	KNO_2-$NaNO_3$	149	89	45
8	R601	KNO_2-$NaNO_3$	149	89	70
9	R601	KNO_3-$NaNO_3$-$NaNO_2$	142	82	45
10	R601	KNO_3-$NaNO_3$-$NaNO_2$	142	82	70

As can be seen, the Aalborg case study includes 32 different combinations, while for Ispaster there are only 10 potential scenarios. The difference comes from the relative low evaporator temperature in the case of Ispaster, that limits the number of PCM materials, while in the case of Aalborg, due to the use of high temperature waste as heat source such limitation doesn't exists.

2.5. System sizing

The sizing of the CHEST system is strongly dependent on the refrigerant used in the HP and ORC loops; in fact, this is seen as one of the most relevant issues in the refrigerant selection since it has a strong impact on the system first costs and the overall financial feasibility of the CHEST system.

In CHESTER D4.2, it was pointed out that the balancing market is the main mechanism of the electrical market where an electrical storage system can offer services to the electrical grid. It is also explained there that the balancing market is in a standardisation process in Europe, and that, although the technical constraints of the rules in order to participate in such markets are in the present very diverse country-wise, they will converge in the near future to standardise electrical grid products. Among the conditions for participating in the balancing market, the minimum electrical power consumed or absorbed from the grid is one of the requisites, and although there is an uncertainty in the short time limit value for such magnitude in the electrical market, we consider within CHESTER WP4 that 1 MW is a convenient hypothesis for the minimum system capacity to be required by the NEMO at country level.

This is the starting point for the system sizing within T4.4 simulation work. Also, it is known from D2.2 that the ratio of the HP capacity and the ORC capacity should have a value of approximately 2, in the case that Butene is used as refrigerant and KNO_3-$LiNO_3$ is used as the PCM storage material. Finally, a third condition for sizing the system is that, within a 1-year period (which is the simulation time frame used), the total energy delivered to the PCM storage is the same as the energy discharged from the PCM storage. We can analytically represent the energy input into the PCM storage from the HP as:

$$Q_{in} = nh_{HP} \cdot COP_{HP} \cdot RLS_{HP} \cdot P_{HP}$$

Where

Q_{in} is the energy input to the PCM storage

nh_{HP} is the number of operating hours of the HP in the period

COP_{HP} is the COP of the heat pump

RLS_{HP} is the ratio of latent heat to the PCM of the total heat generated by the HP

P_{HP} is the electrical power of the heat pump

Similarly, for the energy retrieved from the PCM storage, we have the following expression:

$$Q_{out} = nh_{ORC}/\eta_{ORC} \cdot RLS_{ORC} \cdot P_{ORC}$$

Where

Q_{out} is the energy output from the PCM storage

nh_{ORC} is the number of operating hours of the ORC in the period

η_{ORC} is the efficiency of the ORC

RLS_{ORC} is the ratio of latent heat to the PCM of the total heat absorbed by the ORC

P_{ORC} is the electrical power of the ORC expander

Since, in a wide time period as can be one year, the energy in and out (disregarding thermal losses from the storage, which should be small enough due to an appropriate storage insulation) should be the same, we can equate both quantities Q_{in} and Q_{out} defined above to get:

$$nh_{HP} \cdot COP_{HP} \cdot RLS_{HP} \cdot P_{HP} = nh_{ORC}/\eta_{ORC} \cdot RLS_{ORC} \cdot P_{ORC}$$

Since we know that for the case of butene with KNO_3-$LiNO_3$ the optimal ratio of the heat pump electrical power to ORC electrical power should be 2, we can deduce the ratio of the number of operating hours for 1 year at both loops substituting this relation into the previous equation:

$$\frac{P_{HP}}{P_{ORC}} = 2$$

$$2 \cdot nh_{HP} \cdot COP_{HP} \cdot RLS_{HP} \cdot= nh_{ORC}/\eta_{ORC} \cdot RLS_{ORC}$$

For this particular combination of PCM and refrigerant, we assume:

$COP_{HP} = 5.16$

$RLS_{HP} = 0.554$

$\eta_{ORC} = 0.138$

$RLS_{ORC} = 0.526$

By substituting this values in the previous equation, we find the following relation for the operating hours in yearly basis for an optimal sizing:

$$\frac{nh_{HP}}{nh_{ORC}} = 1.5$$

This is basically a characteristic of the electrical market prices distribution; it is only an approximation, but is accurate enough for the preliminary sizing of the simulations of different combinations of PCM and refrigerants in T4.4.

Going back to the equations for Q_{in} and Q_{out} from the PCM storage, we equalise again and substitute this ratio of 1.5 operating hours in yearly basis for each loop:

$$1.5 \cdot COP_{HP} \cdot RLS_{HP} \cdot P_{HP} = RLS_{ORC} \cdot P_{ORC}/\eta_{ORC}$$

Now, we consider the minimum electrical capacity required for participating in the balancing market mentioned before. Since we assume a minimum value of 1MW, and in general, the capacity of the HP should be bigger than the ORC capacity, we set the power of the ORC to 1 MW. In case of fixing the HP instead of the ORC, the conclusions would be equivalent, as well as if any other minimum capacity value was considered. With these assumptions, we have that the HP capacity will depend on the latent fraction in both loops, the ORC efficiency and the HP COP as:

$$P_{HP} = RLS_{ORC}/(1.5 \cdot COP_{HP} \cdot RLS_{HP} \cdot \eta_{ORC})$$

Due to the fact that we have fixed the ORC generating capacity to 1 MW, and the operating hours are fixed, the smaller the power of the heat pump, the smaller the system will be for producing the same amount of electricity. In other words, a higher the system efficiency implies a smaller capacity, but also a smaller amount of electricity has to be purchased to generate the same amount of energy. This fact has strong implications on the system economic balance, as will be shown in section 3.

The implications extend also to the sizing of the PCM storage. Intuitively, the higher the ORC efficiency is, the smaller will be the amount of energy to be retrieved from the PCM storage to produce the same amount of electricity. If we need less energy from the PCM storage, its volume will be smaller, which implies a reduction of the storage investment costs.

In order to size the PCM storage, we take into account that the ratio of the PCM bulk volume per unit length of the PCM storage HX cannot be set completely independent one from the other. In the current analysis, we use a value of 5 litres of PCM storage per each meter of HX embedded in the store. First, the PCM storage HX power is set as the maximum of the requirements from the HP and ORC loop capacities:

$$P_{HX} = MAX(COP_{HP} \cdot RLS_{HP} \cdot P_{HP};\ nh_{ORC}, RLS_{ORC} \cdot \frac{P_{ORC}}{\eta_{ORC}})$$

With this, the total length of the PCM heat exchanger is calculated by:

$$P_{HX} = h_{eff} \cdot Area \cdot \Delta T = h_{eff} \cdot (\pi d_i^2 \cdot L/4) \cdot \Delta T$$

$$L = \frac{4 \cdot P_{HX}}{h_{eff} \cdot \pi d_i^2 \cdot L \cdot \Delta T}$$

Where:

P_{HX} is the PCM storage heat exchanger power

h_{eff} is the effective heat transfer coefficient; the effective heat transfer coefficient is calculated based on the Shah correlation for condensation/evaporation and corrected by the PCM Biot number. See D4.2 for further details on this quantity.

L is the total pipe length of the PCM heat exchanger

d_i is the heat exchanger pipes inner diameter

For the sizing of the storage in the simulations, we assume a heat exchanger with pipes with inner diameter of 20 mm, the effective heat transfer coefficient is assumed to be 80 W/m^2·K, and the temperature difference during the simulations is set to be 5 K. All these values are used only for sizing purposes: dynamic values calculated by the TRNSYS model are used during the simulations at each time step. Finally, the volume of the PCM storage, is calculated as

$$Vol_{PCM} = PCM\_to\_HX \cdot L$$

Where

PCM_to_HX is the ratio of PCM material per unit length of PCM heat exchanger, in m^3/m

L is the total heat exchanger length in m

The relevant point of this procedure is the recognition that the refrigerant and PCM selection of the CHEST system implies different sizes of the different components of the CHEST for the same electrical storage performance (represented here indirectly by the constant electrical power of the ORC and the same number of operating hours imposed on the calculations). This is mainly driven by the specific efficiency of the ORC and heat pump COP, and the latent ratio of each of the cycles, and all these quantities are dependent on the refrigerant properties as well as the PCM melting temperature, which establishes the temperature level of the CHEST thermodynamic cycles. In section 3, we will come back to the implications of the materials selection on the system sizing.

3. Selection of PCM/refrigerant

3.1. Performance assessment metrics

For the comparison of the different combinations of PCM and refrigerant, we use the simulation results for each case analysed. There are a lot of results from the simulations, but in order to simplify the assessment, we will focus on the following variables:

1. System sizing: the different combinations require different capacities of the elements, due to differences in COP and ORC efficiency, among others. This has strong implications on the investment costs.
2. Operation profit: The balance associated with the system electrical storage service, which only takes into account the economics of the purchased and sold electricity. The control strategy is not optimized, instead is a conservative approach to ensure similar number of operating hours in each case allowing for a better comparison among the different materials.
3. Heat requirement: In general, the CHEST system acting as an electrical storage is a net heat consumer, and each combination yield different heat requirements for the same electrical output

3.2. Aalborg case study

Aalborg is located in the Northern part of the Jutland Peninsula in Denmark. It is Denmark's 4th largest city with a population of 114,000 (as of 2018). Most of the city is supplied by a DH network, which is managed by the municipally-owned utility company Aalborg Forsyning. In 2016, 98 % of heated buildings within the area covered by the DH network were connected to the network, for a total number of 36,716 customers. Multiple-apartment buildings are counted as a single customer, so the number of households supplied by the DH network is higher than the number of customers. Most of the heat demand occurs in the period October-May, as there is much less space heating demand between May and September.

A large cement producer, Aalborg Portland, is located just outside the city and supplies the DH network with large amounts of industrial excess heat. Additionally, Aalborg has a waste incineration combined heat and power (CHP) plant and a large coal-fired CHP power plant, both of which supply heat to the DH network and electricity to the electrical grid. A detailed description of the Aalborg case study can be found in CHESTER D2.1

The availability of waste heat from several resources, as well as a noticeable heat demand through the DH network, make a great foundation for a feasible implementation of the CHEST system linked to the existing infrastructure. The waste heat has an excellent temperature level, thus allowing a high evaporator temperature of the heat pump, which opens the possibility of keeping the heat temperature lift small enough to ensure a high heat pump COP, or increase the condensing temperature at the PCM store, which will benefit the ORC efficiency. Whatever the most appropriate strategy might be, the high temperature level of the waste heat offers high flexibility in regards of system design.

In this case, 32 different scenarios where simulated as listed in table 4 in section 2.4. These scenarios cover 12 different refrigerants and 8 PCM materials, sampled according to the characteristics of the refrigerant critical temperature and PCM melting temperature as described in section 2.4. A selection of the main results is presented hereunder.

The first result shown in figure 1 is the boxplot showing the distribution of heat pump power required for a 1 MW ORC expander as a function of the refrigerant selected for the CHEST system. The distribution shown in the boxplot corresponds to different PCM materials used, that modify the refrigerant performance by changing the operating temperature range.

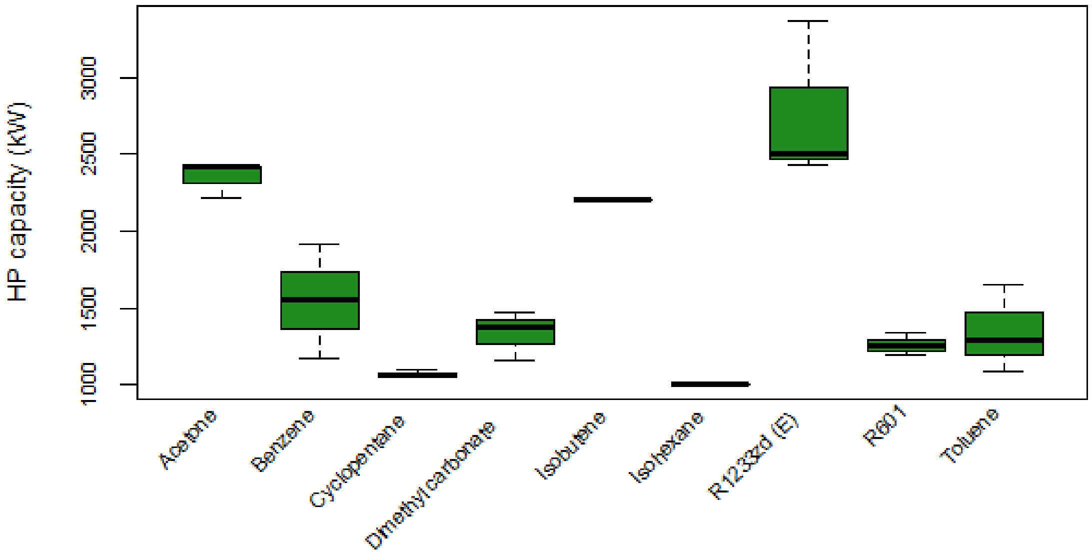

Figure 1: HP capacity required for a 1 MW ORC as a function of the refrigerant

The results show differences up to 300% in terms of required heat pump capacity to produce the same amount of electricity by the ORC, with hydrocarbons like hexane and pentanes performing better than the rest. This implies a significant reduction on the first costs of the CHEST system, since the HP capacity has implications also on the PCM storage required. This can be seen in the figure 2, where the same boxplot is reproduced, but instead of the HP capacity we show the distribution of PCM mass required in each scenario.

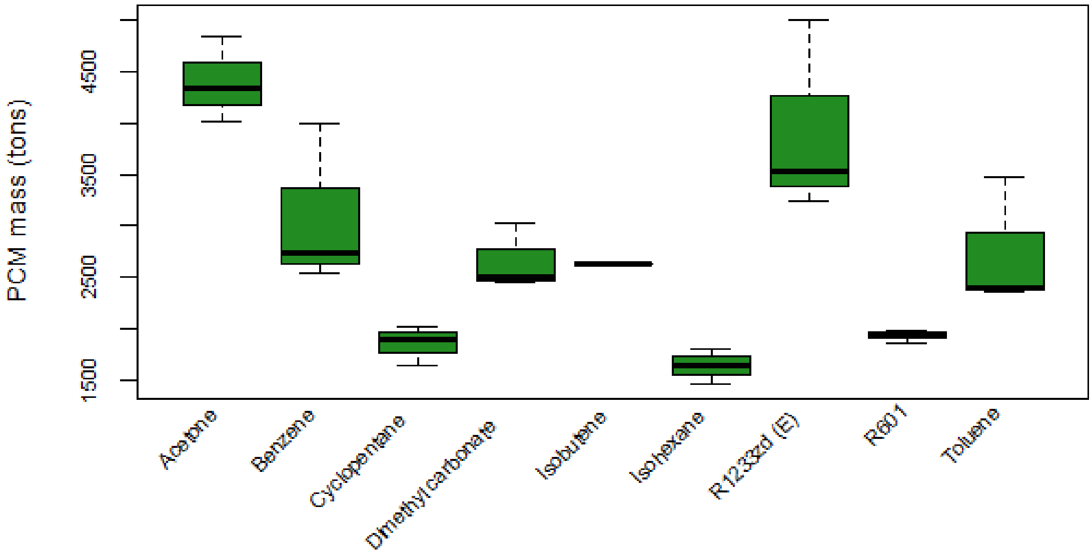

Figure 2:PCM mass required for a 1 MW ORC as a function of the refrigerant

When looking at figure 2, we see even stronger differences among the best performing refrigerants. Again, the hydrocarbons are the most appealing refrigerants, but some of them like toluene or benzene, that showed similar performance to hexane or pentane in terms of HP capacity lag farther in terms of PCM requirements. Again, this has an impact in the investment costs, since according to table 2 the cost of PCM material is roughly in the range of 300 to 2000 € per ton.

We look now to the operation profit associated with the system operation in the different simulations. Note that the specific values of the operation profit are not representative of the CHEST potential, due to the fact that the system operation is very conservative: as explained before, the operation strategy is far from optimal, since we want to ensure a similar number of operating hours of the CHEST in each simulation. Besides, the data on energy prices used for the simulations is from the danish market in the year 2016, and the danish balancing market prices are caped to a bonus respect the spot market [12], which is not the most favorable market condition for the CHEST system. However, the relative score of each simulation is useful for the comparison of the different refrigerant/PCM combinations. In figure 3 we can see the operation profit results in each case. The box and bars in the boxplot show the distribution of the results for all PCMs considered for all refrigerants

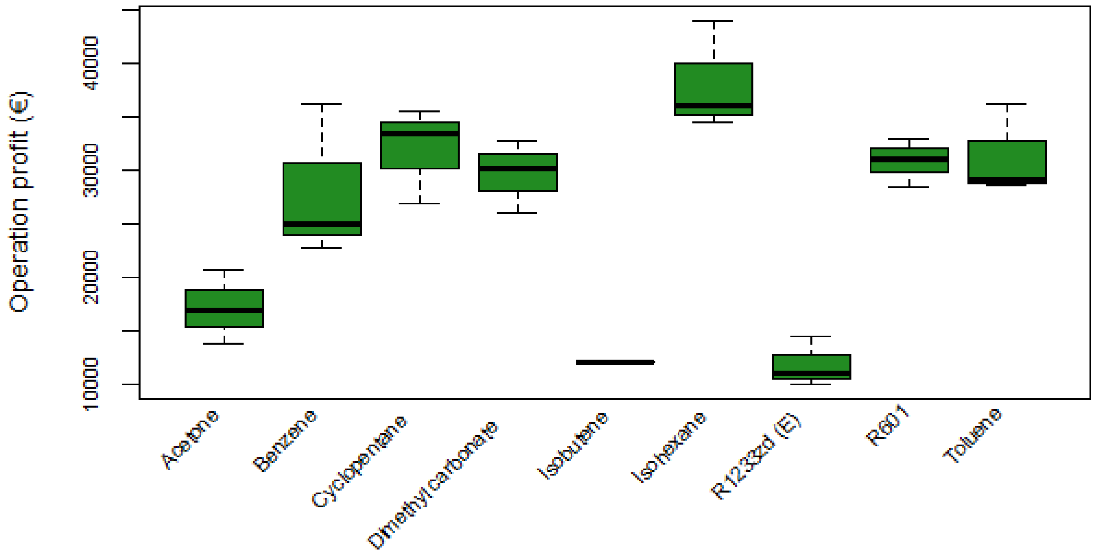

Figure 3: Yearly operation profit for different refrigerants for 1 MW ORC

There are huge differences among the refrigerant/PCM combinations analysed, of over 400% from the worst scenario to the better. Again, hydrocarbons are the better option, with isohexane leading the list of scenarios with highest operation profit. In order to see the effect of the PCM selection on the operation profit, we see in the figure 4 the dependence of the operation profit in the PCM melting temperature, since it is the most decisive of all the PCM material properties

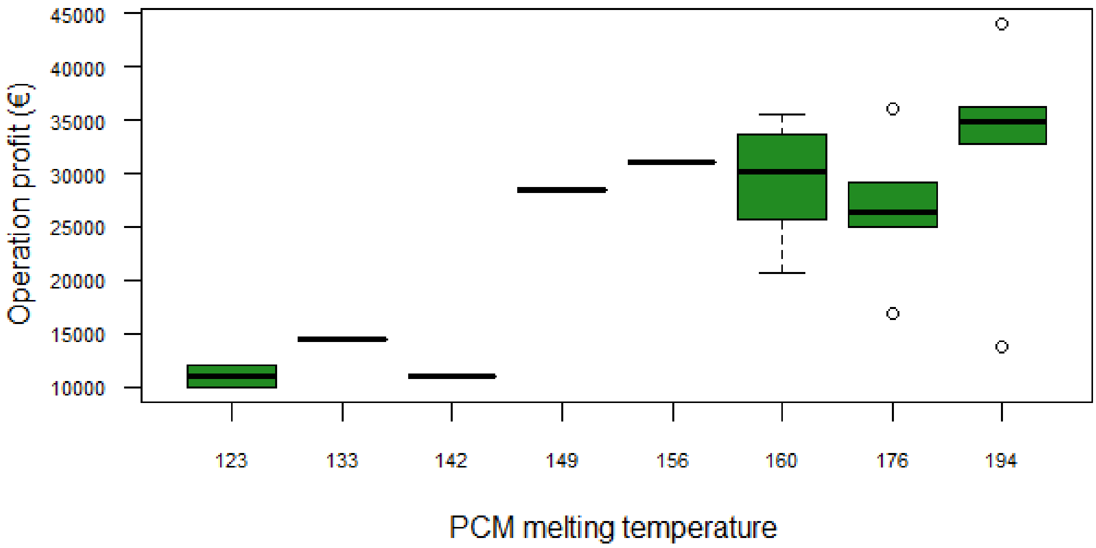

Figure 4: Yearly operation profit as a function of the PCM melting temperature for 1 MW ORC

The previous figure shows that there is a tendency of increasing operation profit as the PCM melting temperature grows. This is related with the increased efficiency of the ORC , but there are other factors affecting the system performance as shown by the vertical dispersion of the values at each temperature level. We can represent the data indicating the values of the refrigerant in each simulation, as can be seen in figure 5:

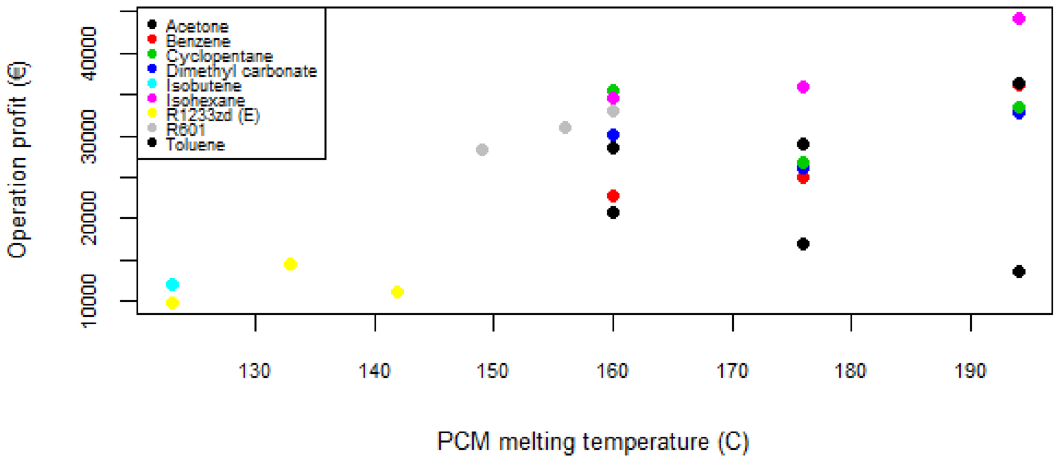

Figure 5: Yearly operation profit as a function of the PCM melting temperature for 1 MW ORC for different refrigerants

Figure 5 shows that there is a consistent sorting of the refrigerants for a given melting temperature, with dry refrigerants showing the best performance, followed by the isentropic refrigerants and finally the wet ones (although only Acetone is a wet fluid among those present in figure 5). This classification of the refrigerants is based in the derivative of the entropy of the saturation line with temperature, and in terms of the model used, affects the condensing temperature affordable by the ORC. This effect can be seen in figure 6, where the operation profit is plotted against the ORC condensing temperature:

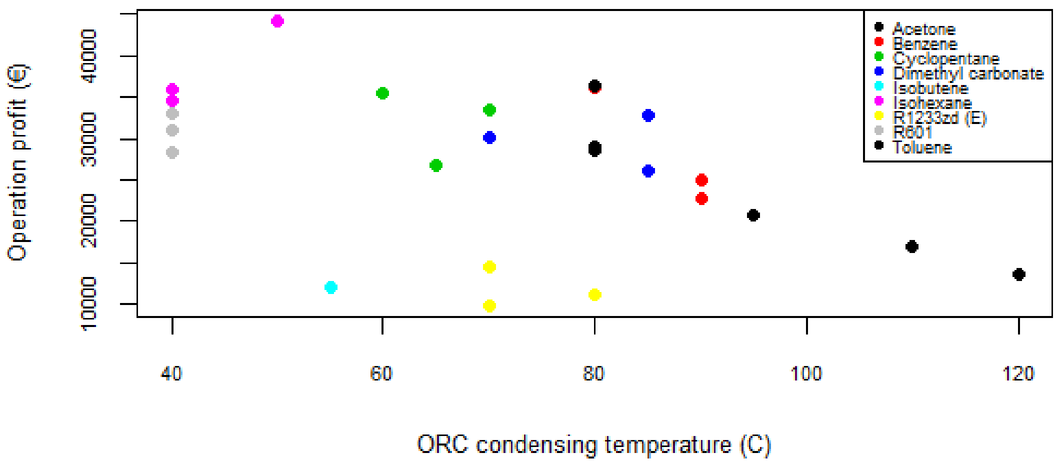

Figure 6: Operation profit as a function of the ORC condensing temperature for 1 MW ORC for different refrigerants

As expected, a smaller condensing temperature, which implies a higher ORC efficiency, is related with a better economic exploitation of the system, although there are cases that seem to break the tendency, this is mostly related with simulations with smaller melting temperatures (see Figure 4).

Finally, to compare the different scenarios, we look at the heat demand resulting in each simulation. Figure 7 plots the system operation profit as a function of the system heat balance. The heat balance is the sum of all the heat delivered by the system (ORC condenser to DH consumption and HP subcooler) minus the heat consumption of the system (HP evaporator and preheater). Hence, a negative value indicates that the CHEST system is a net heat consumer, while a positive value indicates that extra heat is generated after the service of electrical storage.

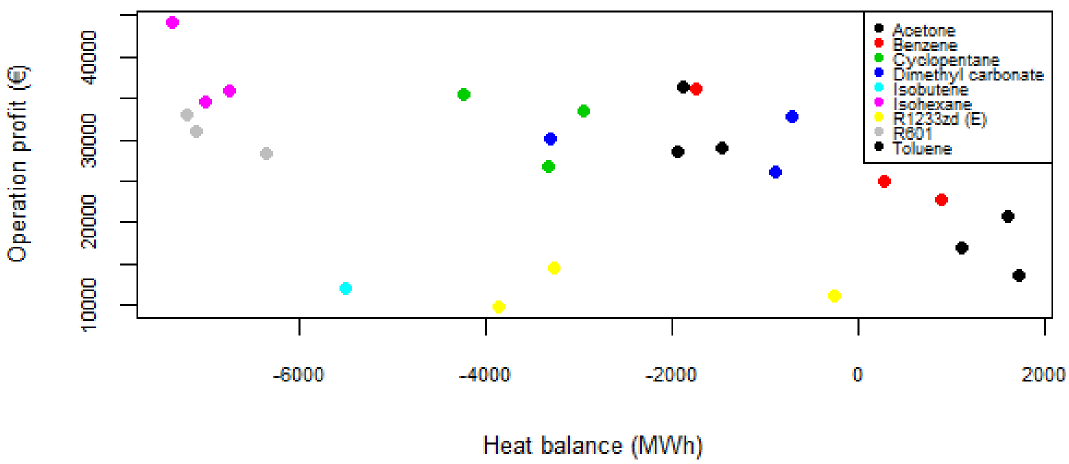

Figure 7: Operation profit as a function of the system heat balance for 1 MW ORC for different refrigerants

The plot shows a general linear tendency between consumed heat and operation profit generated. Note that the operation profit does not take into account any costs nor revenues generated by the heat sold or consumed, it is just originated by the service as electrical storage. This has implications in the services offered by the CHEST system, since the maximization of the benefits associated with the electrical storage seems to reduce the potential for heat services. To have a clearer picture, we show the operation profit for each of the simulations as a function of the heat consumed at the HP evaporator in Figure 8. Although in this analysis the cost of the heat has been ignored, it is interesting to minimize, if possible, the heat required by the system:

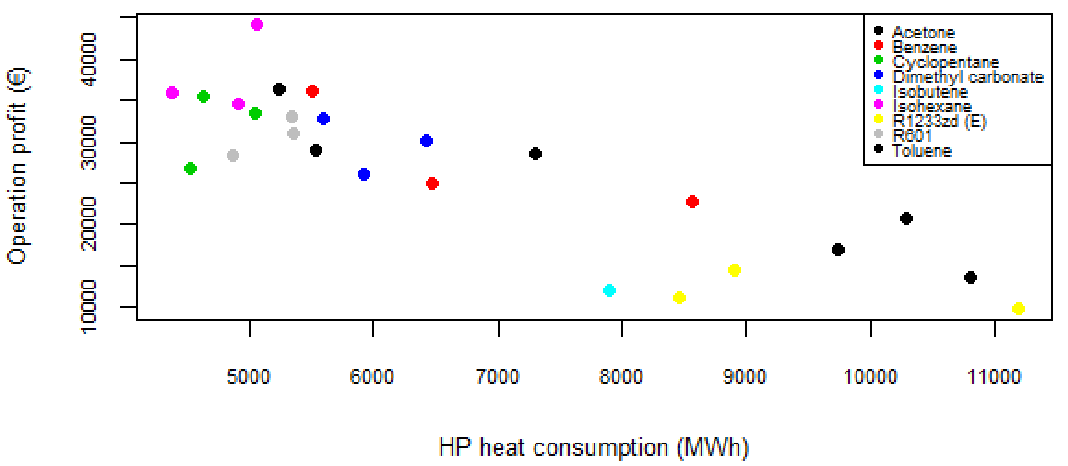

Figure 8: Operation profit as a function of the HP evaporator heat consumprion for 1 MW ORC for different refrigerants

Here we see a nice tendency, with the best results aligned with the smaller consumption. The main reason is that the most efficient refrigerant/PCM combinations are characterised by a smaller size of the HP for the same electricity production. This means that less heat needs to be pumped to the PCM storage to produce the same amount of electricity.

An important driver of the heat demand is the latent heat ratio of the HP and ORC loops. This is defined as the fraction of heat of each loop that is delivered in latent form (in other words, which is delivered or retrieved from the PCM) to the total heat generated or absorbed by the HP or the ORC, respectively. A value of 1 for the heat pump loop means that all the heat generated by the HP will be delivered to the PCM, and in the case of the ORC loop , a value of 1 means that all the heat to the ORC generator would come from the PCM storage. The next figure shows the total heat balance of the CHEST system as a function of the HP and ORC loops latent ratio:

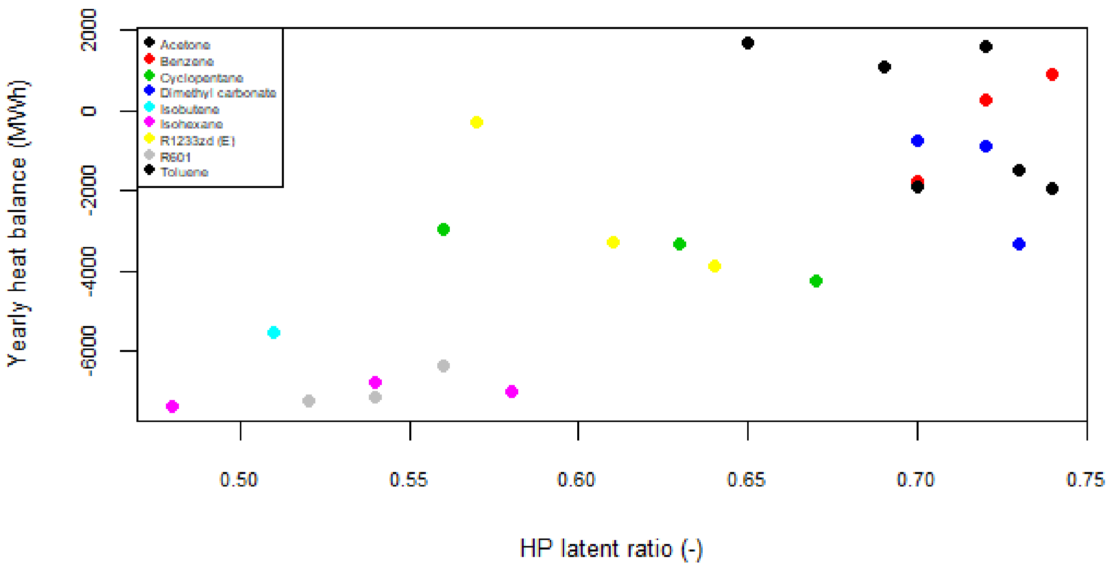

Figure 9: Yearly heat balance as a function of the HP latent ratio for 1 MW ORC for different refrigerants

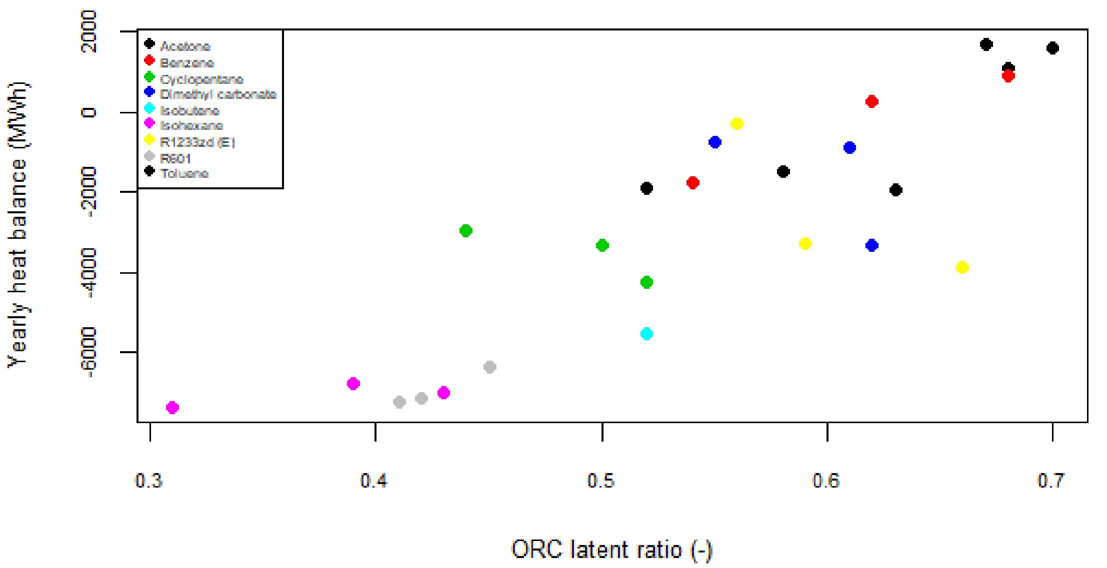

Figure 10: Yearly heat balance as a function of the ORC latent ratio for 1 MW ORC for different refrigerants

It gets clear from the previous figures that the higher the latent ratio of any of the loops, less heat will be required to drive the CHEST system. However, recall also from Figure 7 that the heat balance is inversely related with the operation profit when operating as an electrical storage, so an equilibrium should be found here and no extreme values are recommended, instead, an intermediate value might probably be the best option.

Based on the results presented in this section, several conclusions can be drawn for the exploitation of the CHEST system under the boundary conditions of the Aalborg case study:

- The selection of the refrigerant and PCM material of the CHEST system has a huge impact on the system performance and costs. Differences in operation profit of up to 300 % among different options are reported, as well as differences of 200 % on investment associated with the HP loop and the PCM storage first costs.
- There are several combinations that show comparable performance, but there appears to be a systematic improvement on the system performance with increasing PCM melting temperatures.
- The electrical storage services compete with the heat services: the better the economic balance of the system, the higher becomes the heat requirement.
- Most of the scenarios analysed show a net heat requirement in order to operate the CHEST system, thus a relevant contribution to heat services might be difficult to accomplish.

Beyond those general conclusions, it is necessary to select the most appropriate combination of refrigerant and PCM material to continue with the analysis foreseen in WP4, since as shown here, it will significantly affect the potential of the CHEST system. As mentioned before, several combinations have a similar performance, but the preferred one would be to use Cyclopentane as refrigerant and $LiNO_3$-$NaNO_3$-KCl as PCM material, that has a melting temperature of 160 C. The reasons for choosing this combination are:

- Relatively small installed capacity when compared to other combinations, which implies a significant reduction in the investment of the CHEST system.
- Relatively high operation profit, due to the reduced HP capacity required and the good ORC efficiency
- Relatively low heat demand among the combinations with better economic performance due to the high latent ratio of the HP and ORC loops
- State of the art working fluid for ORC and HP applications
- Temperature level high but still on the limit of the state of the art of commercial heat pumps
- No limitations known for the PCM due to flammability, toxicity or long-term stability.

In the upcoming work within WP4, further optimisation of the CHEST system for the Aalborg case study will be carried on. This will rely mainly on the scheduling optimisation, that will allow to have a realistic evaluation of the system potential due to the associated improvements in economic figures, and this analysis will be done with the selected refrigerant and PCM material.

3.3. Ispaster case study

In the small town of Ispaster (about 700 inhabitants), which is located in the Basque country about 50 km northeast of Bilbao, Spain, several (public) buildings are connected to a DH network and to an electrical micro-grid. This part of the town, with an annual gross heat demand of about 108.4 MWh and an annual electricity demand of about 23.5 MWh, is considered in the Ispaster case study. A detailed description of the Ispaster case study can be found in CHESTER D2.1.

Renewable electricity is locally generated by PV panels. In case the PV electricity generation is higher than the current electricity demand of the buildings in the electrical micro-grid, this surplus of PV electricity can be used to drive the HP and charge the HTTES of a CHEST system. Accordingly, when the PV electricity generation is lower than the current electricity demand of the buildings in the electrical micro-grid, the HTTES of the CHEST system can be discharged in order to drive the ORC and provide electricity to the electrical micro-grid. If the HTTES of the CHEST system is completely discharged, the remaining electricity demand has to be covered by the purchase of electricity from the distribution system operator (DSO).

The heat demand of the DH network is covered on the one hand by solar thermal collectors and on the other hand by a wood chips boiler. This means that all the heat is already generated by renewables.

In contrast to Aalborg case study with the availability of high temperature waste heat, here in Ispaster, the use of solar thermal collectors as a heat source limits the potential scenarios concerning PCM/refrigerant combinations stronger. The reason is that solar thermal collectors work more efficiently at lower fluid temperatures. Therefore, it is not reasonable to allow for high HP evaporator temperatures, because this will reduce the solar thermal yield and will thus lead to an increased demand of biomass (= wood chips).

As a consequence of this, it was decided to analyze only 10 potential scenarios concerning PCM/refrigerant combination and concerning HP evaporation and ORC condensation temperature level. As you can see from Table 6 in Chapter 2.4, the analysis comprised 3 refrigerants, R1233zd(E), Isobutene and R601, and 4 PCMs being the ones with the lower melting temperatures. Besides, variation was done for the HP evaporation temperature level (which affects the COP, but also the solar thermal yield as mentioned above) and the ORC condensation temperature level (which affects the ORC efficiency and the possibility of transferring heat from the ORC condenser to the DH network).

Furthermore, as will be shown below with the results, it was distinguished between an “Ispaster 2.0” and an “Ispaster Island” case. The “Ispaster 2.0” case considers more or less the situation as it is now in Ispaster regarding the electricity, i.e. regarding the installed PV panels and the need for purchasing the remaining electricity from the DSO. In contrast to that, the “Ispaster Island” case considers an island energy system, i.e. there is no connection to the DSO anymore and thus, PV + the CHEST system must provide electrical self-sufficiency for Ispaster at any point of time. In this case, higher CHEST system sizes are required which affects the selection of the PCM/refrigerant combination as is shown below with the results. A more detailed description of the cases “Ispaster 2.0” and “Ispaster Island” can be found in CHESTER D4.5.

In a first run of simulations, all 10 potential scenarios concerning PCM/refrigerant combination and concerning HP evaporation and ORC condensation temperature level were analyzed for the

"Ispaster 2.0" case. All simulations in this first run were done with a nominal electric power of the ORC expander of 1 kW.

Figure 11shows the required nominal electric HP power (blue column) and the required PCM mass (inner orange column) for a CHEST system with 1 kW ORC expander in "Ispaster 2.0" case. The PCM melting temperature is given in dark blue at the bottom of the columns and the HP evaporation temperature and ORC condensation temperature is given above the columns for each scenario. The scenario numbers given in the figure refer to the ones given in Table 6.

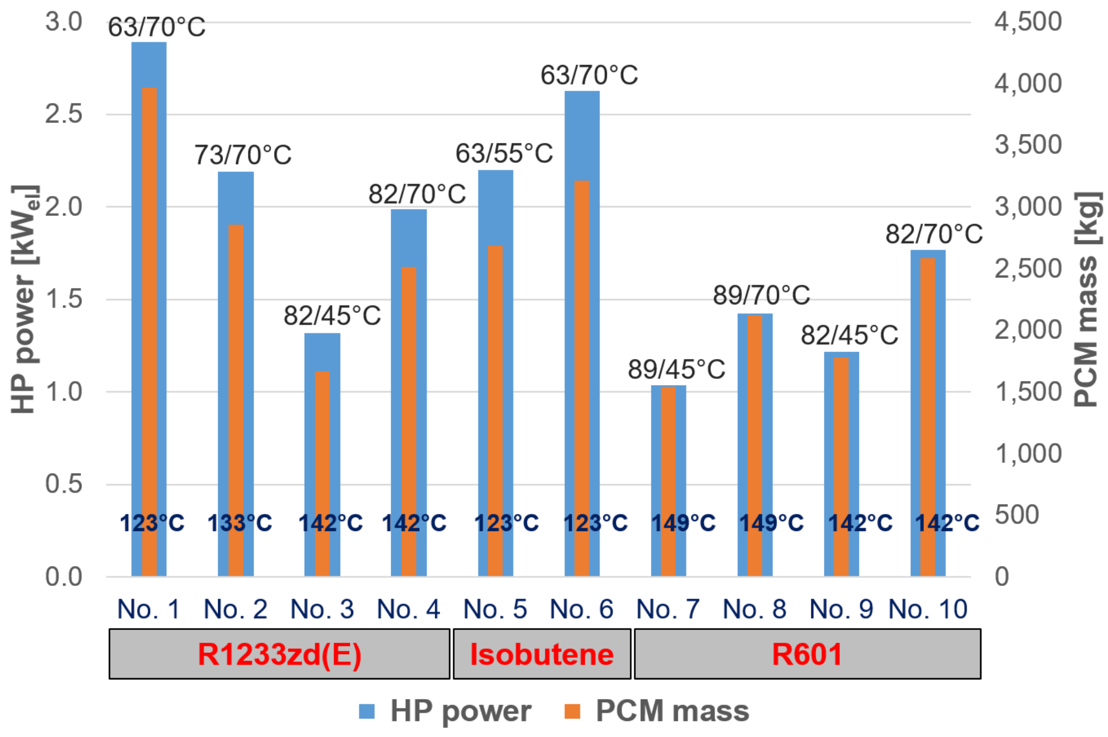

Figure 11: HP nominal electric power and PCM mass required for a CHEST system with 1 kW ORC expander, for different PCM/refrigerant combinations and HP evaporation and ORC condensation temperature levels

First of all, the figure shows that there are significant differences in the required HP sizes and PCM mass for the selected scenarios. Concerning refrigerants, it can be seen that the hydrocarbon R601 leads to generally lower system sizes compared to the other two fluids. Furthermore, there is a considerable influence of the ORC condensation temperature level recognizable from the figure. Namely, applying a low ORC condensation temperature level of 45 °C leads to the lowest required system sizes. This is due to the fact that a low ORC condensation temperature results in a high P2P ratio as can be seen in Figure 12.

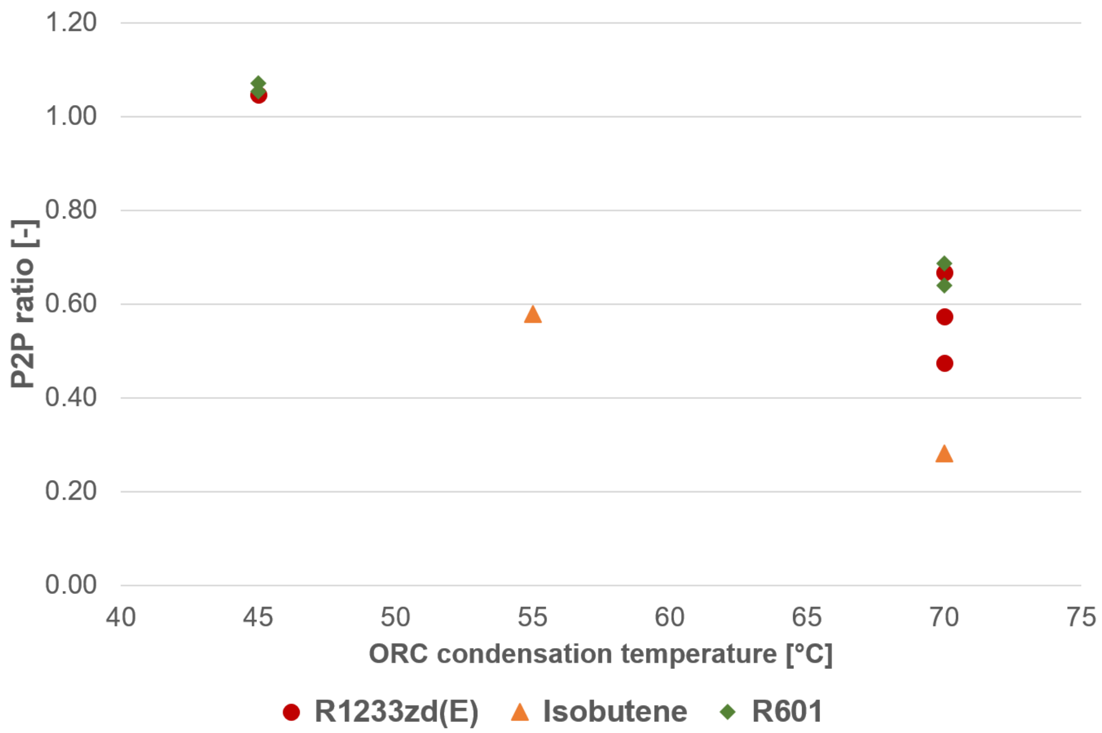

Figure 12: P2P ratio as a function of the ORC condensation temperature for different refrigerants

However, the disadvantage of a condensation temperature of only 45 °C is that this temperature is too low to be able to transfer the ORC condensation heat to the DH network. This results in an increased heat demand as is shown in the following figure where the ORC net electricity generation is plotted vs. the heat balance of the CHEST system. Figure 13 also illustrates that the CHEST system is a net heat consumer for every scenario analyzed here, because the heat balance takes always negative values.

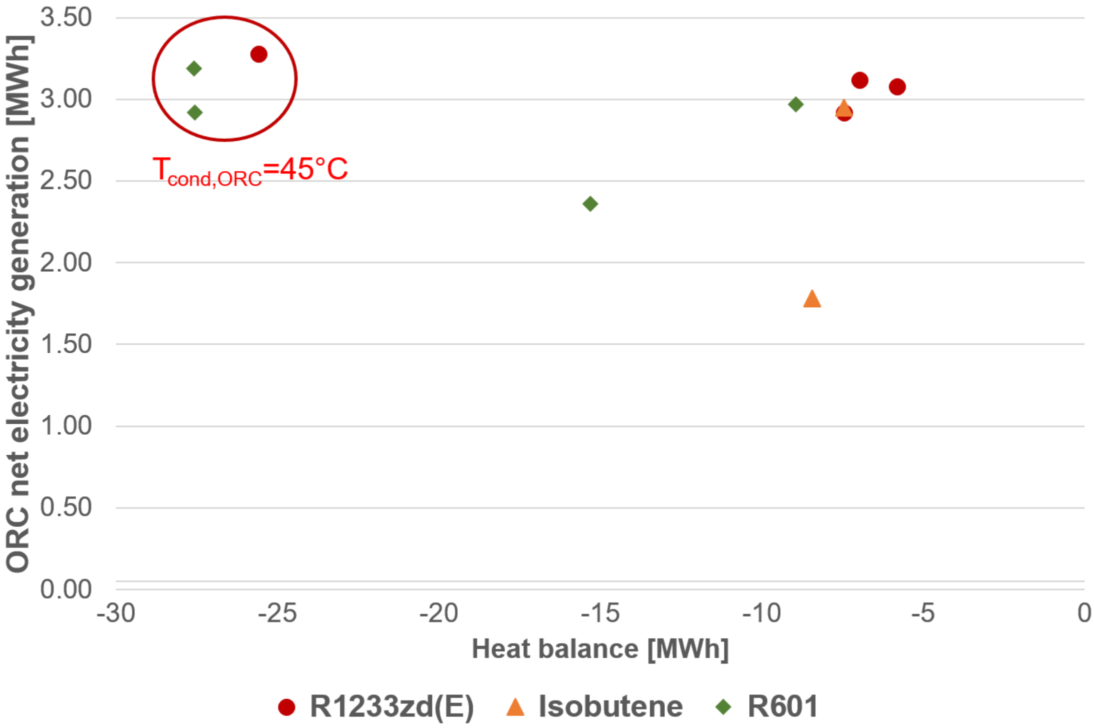

Figure 13: ORC net electricity generation vs. CHEST heat balance for different refrigerants

As will be discussed later more in detail, an increased heat demand also leads to an increased demand of biomass (= wood chips) and thus to an increase of the annual costs. On the one hand, there are costs for the purchase of electricity from the DSO and on the other hand, there are costs for the purchase of wood chips for the boiler.

As the differences in the ORC net electricity generation are not very distinctive for an ORC nominal electric power of 1 kW (see Figure 13), a second run of simulation was done for an ORC nominal electric power of 3 kW. A second effect of this increase of the ORC size is the fact that now, only part of the heat from the ORC condenser is transferred to the DH network (if the ORC condensation temperature allows this at all), because in summer, the heat demand of the DH network is sometimes lower than the available ORC condenser heat. So, carrying out simulations for two different sizes of the ORC changes somewhat the differences between the several scenarios on both the electric and the thermal side.

For the second run of simulations, only the scenarios No. 1-4 and 9+10 from Table 6 were considered due to the following reasons:

- Isobutene was discarded from the further analysis as it shows relatively low performance (cf.Figure 12 + Figure 13) and requires rather high CHEST system sizes (cf. Figure 11).
- For R601, the combination with the PCM KNO_3-$NaNO_3$-$NaNO_2$ (melting temperature of 142 °C) shows slightly better results than the combination with the PCM KNO_2-$NaNO_3$ (melting temperature of 149 °C). Furthermore, the high melting temperature of 149 °C, and as a consequence of this, the higher HP evaporator temperature of 89 °C, results in relatively low solar thermal yields. Therefore, the latter PCM with the higher melting temperature was discarded from the further analysis.

Figure 14shows for this second run of simulations the ORC net electricity generation plotted vs. the heat balance of the CHEST system. For better understanding of the single data points, the scenario numbers from Table 6 are included in this plot. Compared to Figure 13, it can be recognized that due to the larger CHEST system size, the ORC net electricity generation is higher now, but on the other hand, the CHEST heat balance also gets worse. This means as a general trend: the more electricity is generated, the more heat is required.

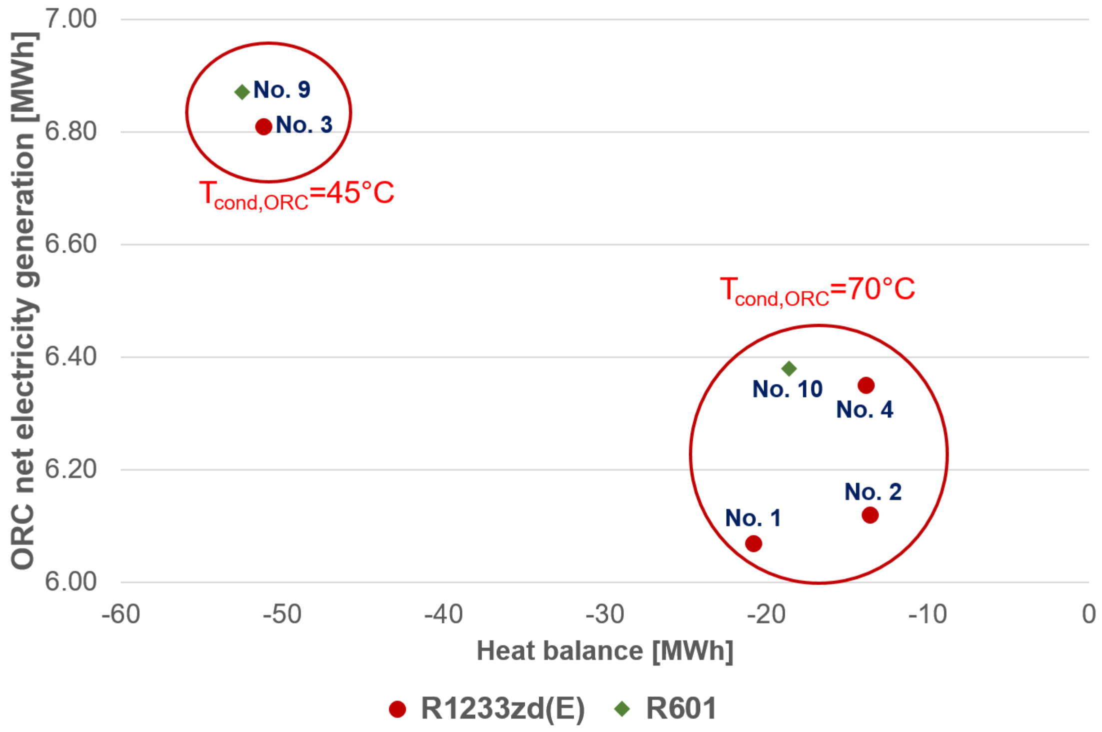

Figure 14: ORC net electricity generation vs. CHEST heat balance for different refrigerants (second run of simulations)

Figure 14clearly shows that applying an ORC condensation temperature of 45 °C results in a higher electricity output of the CHEST system, but this is achieved at the expense of a higher heat demand, compared to the scenarios with an ORC condensation temperature of 70 °C. A higher ORC net electricity generation means that less electricity must be purchased from the DSO, while a worse heat balance means that there is a higher biomass demand. This is shown in Figure 15.

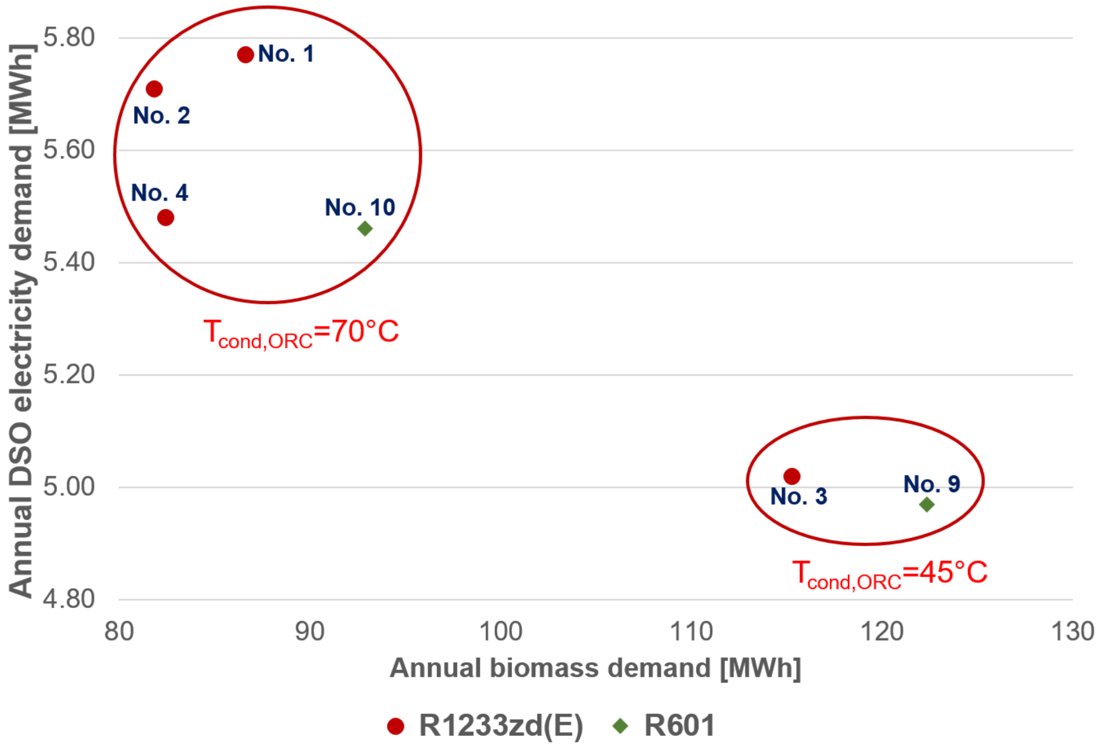

Figure 15: Annual DSO electricity demand vs. annual biomass demand for different refrigerants (second run of simulations)

The demand for purchasing electricity from the DSO and the demand for purchasing biomass for the boiler results in the total annual energy-related costs, which are shown in Figure 16 for the 6 different scenarios considered here. As can be seen from this figure, Scenario No. 4 shows the lowest annual energy-related costs (ca. 2,800 €).

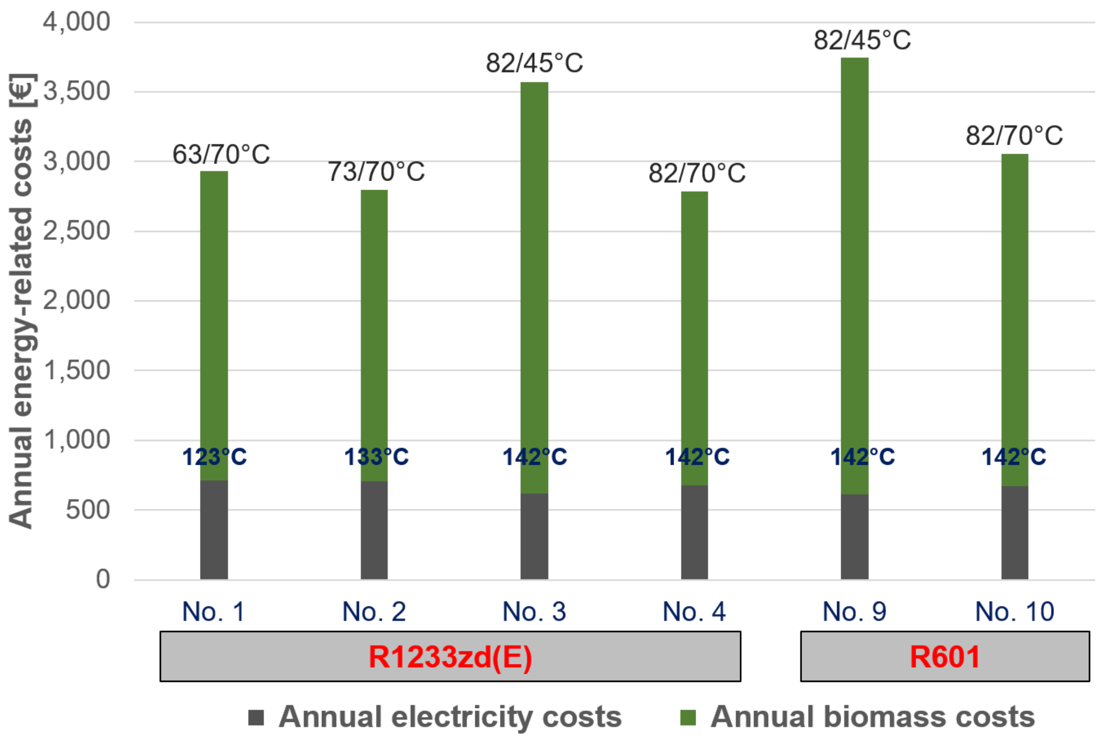

Figure 16: Annual energy-related costs for different refrigerants (second run of simulations)

Regarding the required CHEST system size, Scenario No. 3 results in the lowest system size and thus has the lowest investment costs as is shown in Figure 17. The investment costs were calculated with the help of the component costs that were given in CHESTER D6.2 (costs of the sensible part of the HTTES not included). As the ORC size was the same in all simulations, the investment costs for this component are equal for every scenario. The PCM storage makes up the highest share of the investment costs.

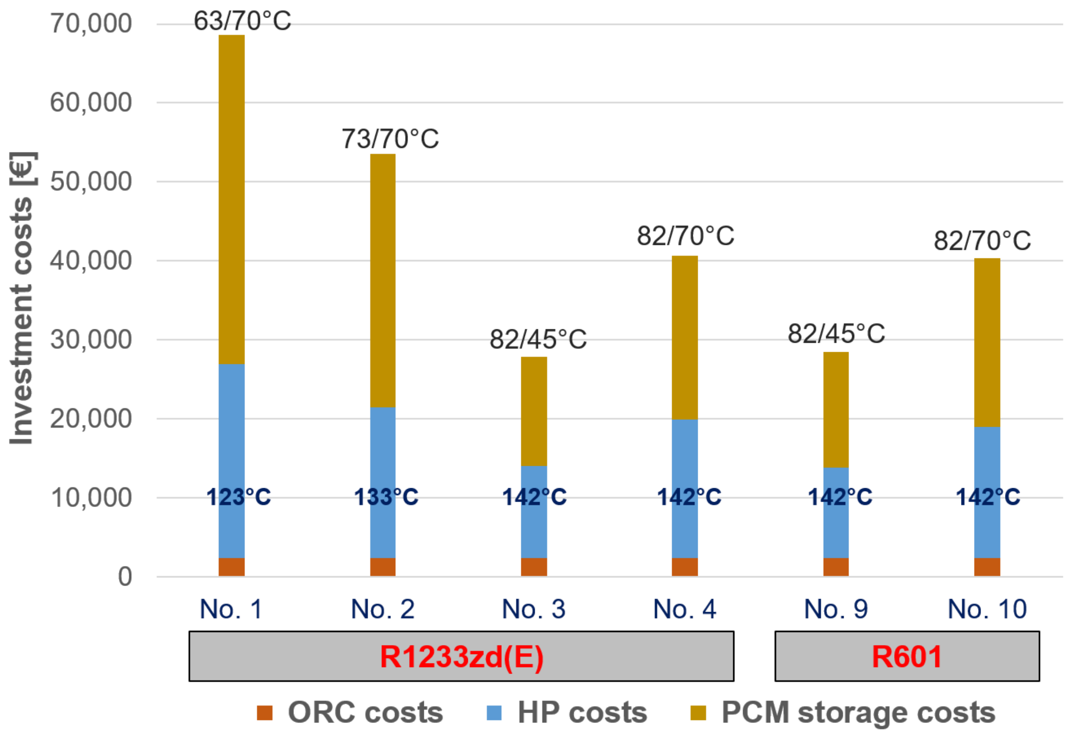

Figure 17: Investment costs for different refrigerants (second run of simulations)

As a conclusion of the two runs of simulations, it was decided to select R1233zd(E) as refrigerant and KNO_3-$NaNO_3$-$NaNO_2$ with a melting temperature of 142 °C as PCM, with 82/70 °C as HP evaporation and ORC condensation temperature levels, respectively (Scenario No. 4), for the further analysis of "Ispaster 2.0" case in WP4. This selection is a good compromise for a satisfying performance concerning both the electric and the heat balance, which results in the lowest annual costs. This selection does not show the lowest investment costs, however, for such rather small CHEST systems (ORC nominal electric power of 1-3 kW), the differences in investment costs are not that high, but they are outweighed by the advantage of lower annual costs.

Another run of simulations was done for the "Ispaster Island" case, because it requires much higher CHEST system sizes, especially as regards to the PCM storage, to achieve electrical self-sufficiency. In this run of simulations, only the scenarios No. 4 (being the preferred one for "Ispaster 2.0" case, see above) and No. 9 (showing the highest P2P ratio and thus expecting the lowest investment costs) were compared with each other.

For such high CHEST system sizes required, the investment costs, and here in particular the PCM storage costs, become the dominating factor for the selection of the most suitable refrigerant/PCM combination. As can be seen in Figure 18, the difference in investment costs for the two scenarios is about 266,000 €, whereas the difference in annual energy-related costs is in the range of just about 1,300 €. Note: The annual electricity costs are zero for both scenarios, because, as stated above, the "Ispaster Island" case considers electrical self-sufficiency, i.e. no electricity is purchased anymore from the DSO.

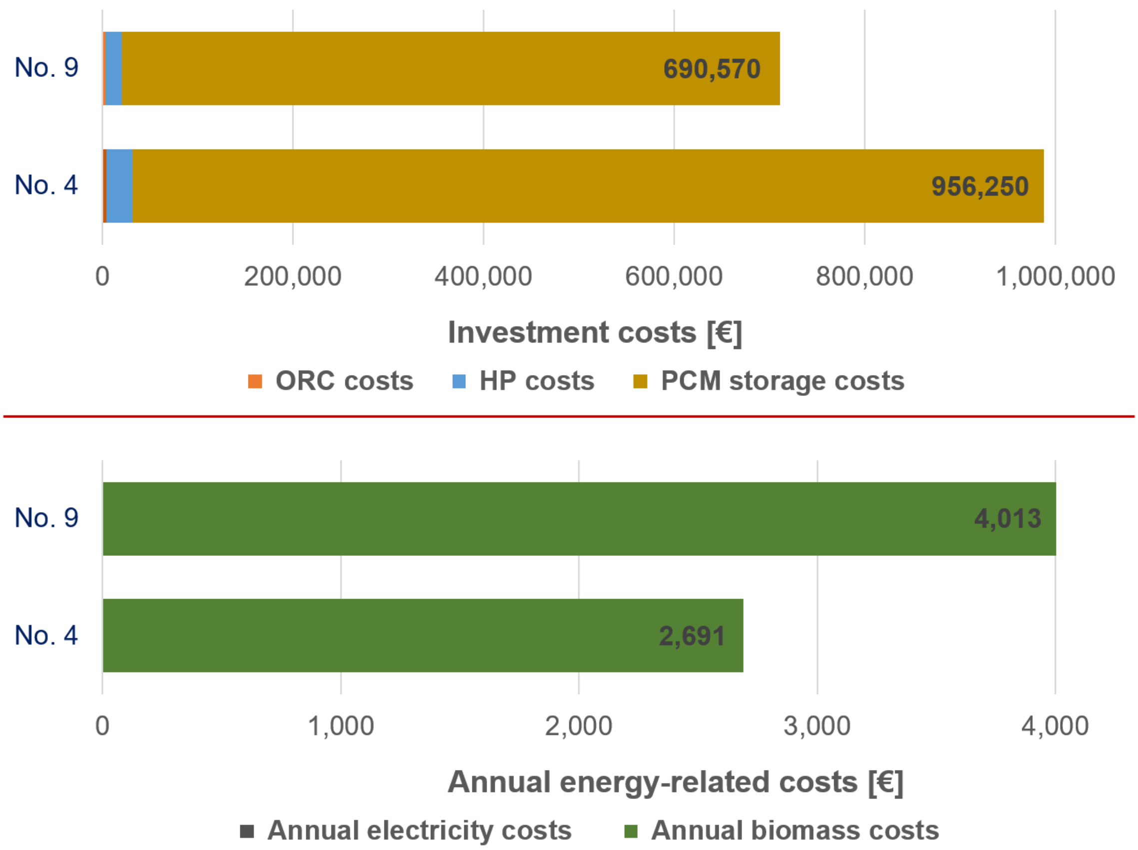

Figure 18: Investment and annual energy-related costs for two different scenarios in "Ispaster Island" case

As a conclusion of this, it was decided to select R601 as refrigerant and KNO_3-$NaNO_3$-$NaNO_2$ with a melting temperature of 142 °C as PCM, with 82/45°C as HP evaporation and ORC condensation temperature levels, respectively (Scenario No. 9).

4. CHEST control strategies

4.1. Introduction

The CHEST system is based on an indirect thermo-chemical storage of electricity: excess electricity from renewable sources together with low grade waste heat is converted by means of a heat pump in higher grade thermal energy and stored in the enthalpy fusion of a medium temperature PCM. This energy can be discharged in the form of electricity or heat, depending on the requirements and the consumers available. The diversity of temperature levels and the possibility of transforming heat on electricity and vice versa makes for a very versatile integration of renewable energy sources, both electrical and thermal. This diversity of operating strategies and services is summarised in the next operating modes, as described in the project proposal. They are represented schematically in figure 11:

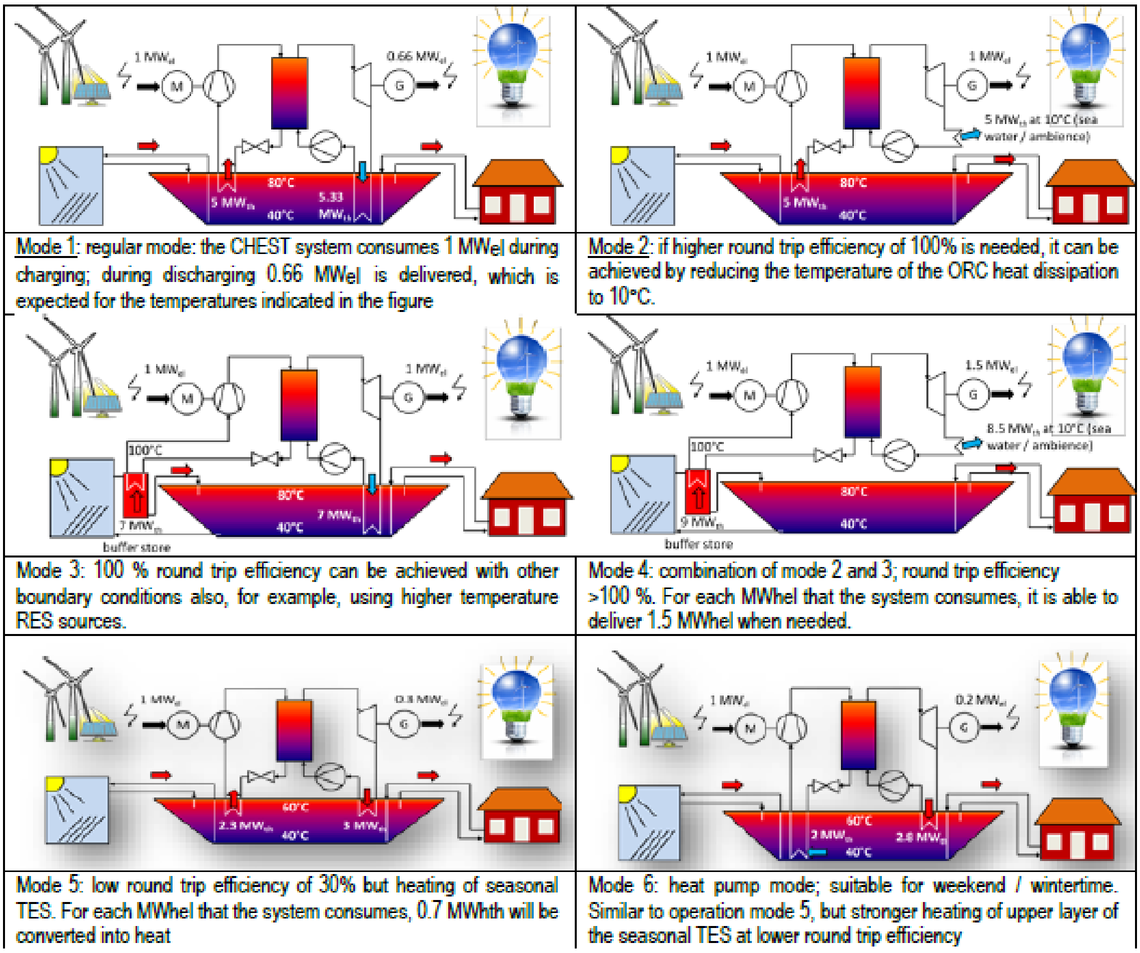

Figure 19: Schematic representation of the CHEST operation modes

It is worth mentioning that the pit storage is not necessary to operate the CHEST system, although it can further improve the integration feasibility. According to [13], from 1980 to 2016, only 39 seasonal storage systems have been deployed in Europe, most of them in Germany and Denmark under the cover of dedicated research programs developed in those countries. Due to this low penetration of seasonal storage, the resulting market potential would be seriously hampered in case the CHEST concept gets limited to this circumstances. Due to this, we will analyze the operation strategies without the inclusion of seasonal storage, even that, as mentioned before, it can improve the integration potential of the CHEST system.

To simplify the interpretation of the CHEST operation modes and give them a wider applicability, the operation modes can be characterized solely by the temperature levels of the source and sink of the CHEST system, which corresponds to the HP evaporator temperature and the ORC condenser temperature. Both of this temperatures have major impact on the system performance and also, on the integration potential; in the case of the HP evaporator, the temperature level limits the technological solutions available, and strongly affects the system overall efficiency, and in the case of the ORC condenser, the temperature level limits the potential use of the residual heat but also affects the system efficiency. Besides, the heat requirements to operate the system, which can be a noticeable added cost to the operation costs.

The analysis of the different control modes of the system requires a new approach for managing the CHEST charge and discharge during the simulations, so an optimizer component was incorporated into the model to manage the charge and discharge control of the system. This modification of the model aims to get a fair comparison of the operation profits associated with the different operation strategies is the system control, or in other words, the criteria for charging and discharging the system depending on the market prices available. This is opposite to the control implemented in the section 3, where we established the control in a way to ensure a comparable number of working hours, to avoid interference of the specific electricity and heat profiles and ensure that the analysis was consequence of the thermophysical properties rather than the specific sizing of the system. Here, a simple optimizer has been developed in TRNSYS and integrated in the model that allows for the scheduling optimization of the system considering the forecasted electrical market prices in a time frame of 36 hours. This makes for a better management of the system, as illustrated graphically in the Figure 14.

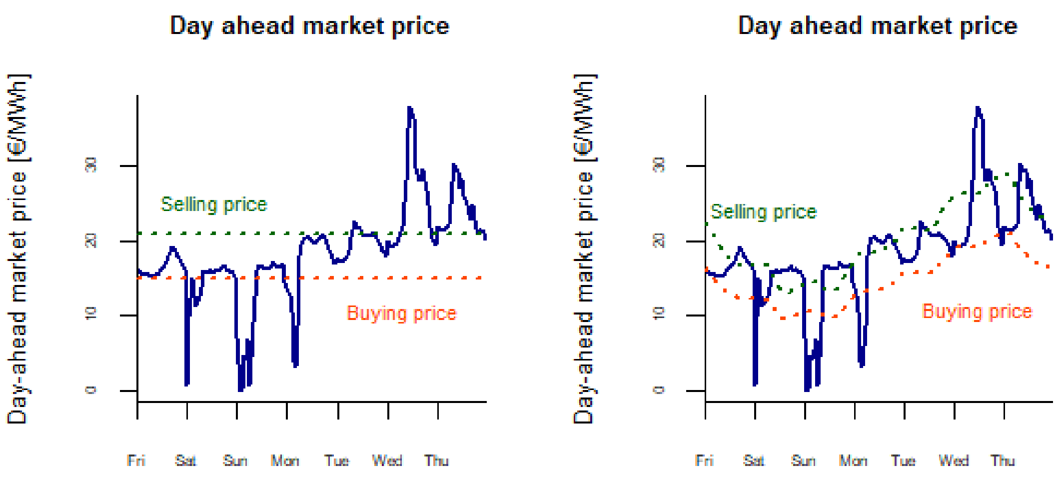

Figure 20: Representation of constant costs operation strategy (left) and optimized control strategy (right)

The two plots in the figure represent in blue the day-ahead market prices and two lines which represent the values used for setting the system either charging (when the market price goes under the market price) and discharging (when the price is higher than the green line, corresponding to higher electricity prices). In the simplest form, a constant threshold value for charging and discharging during a whole week, as seen in the left plot, may miss many running opportunities due to the fact that only charging or discharging happens for several consecutive days, reducing the system capacity factor and penalising the economic potential. On the right-side, a dynamic strategy based on the close future costs is implemented, and this allows for a daily period of charging and discharging, which increases the system profitability. In short, the optimiser is able to cope with daily, weekly and seasonal variations on market prices to maximize the operation profits.

With this upgrade in the T4.2 model, a set of 16 different scenarios for the operation strategies of the CHEST system was defined, corresponding to different temperature levels imposed at the HP evaporator and ORC condensing temperature. Table 5 shows the temperature levels selected at each of them.

Table 7: Values of CHEST source and sink temperature levels

HP Evaporator temperature (°C)	ORC Condenser temperature (°C)
100	95
80	75
60	55
40	35

All values at table 5 are combined to define the scenarios analysed in this section, which will allow to compare the performance of the system under different control strategies.

4.2. Results

The analysis done in this section, as happens with all the research within WP4 is focused on the integration of the CHEST system into the energy networks. Due to this, the simulation work to study the different control strategies of the system is strongly conditioned by the energy prices, in particular, the electricity market prices. The CHEST system integration strategy followed (see D4.2 for the motivation of such approach), assumes that the CHEST operates buying and selling electricity both in the day-ahead market and the balancing market as a replacement reserve asset. The data of the electricity market used in the simulations (day ahead market and replacement reserve up and down) is from the Danish market for the year 2016. This was selected since the data available for the DH at the Aalborg case study is for the year 2016.

The first result we show is the operating time for the HP and ORC for each scenario. We use the capacity factor to represent the operating time, which is defined as:

$$Capacity\ factor\ (CF) = \frac{Yearly\ operating\ hours}{8760} \cdot 100\ [\%]$$

Where the 8760 is the number of hours in a year. The charge capacity factor uses the yearly operating hours of the HP and the discharge capacity factor uses the ORC operating hours. Since there is no possibility to simultaneously charge and discharge the CHEST, the maximum capacity factor for charge and discharge should be close to 50 %. Figure 15 shows the charge capacity factor as a function of the evaporator and condenser temperatures:

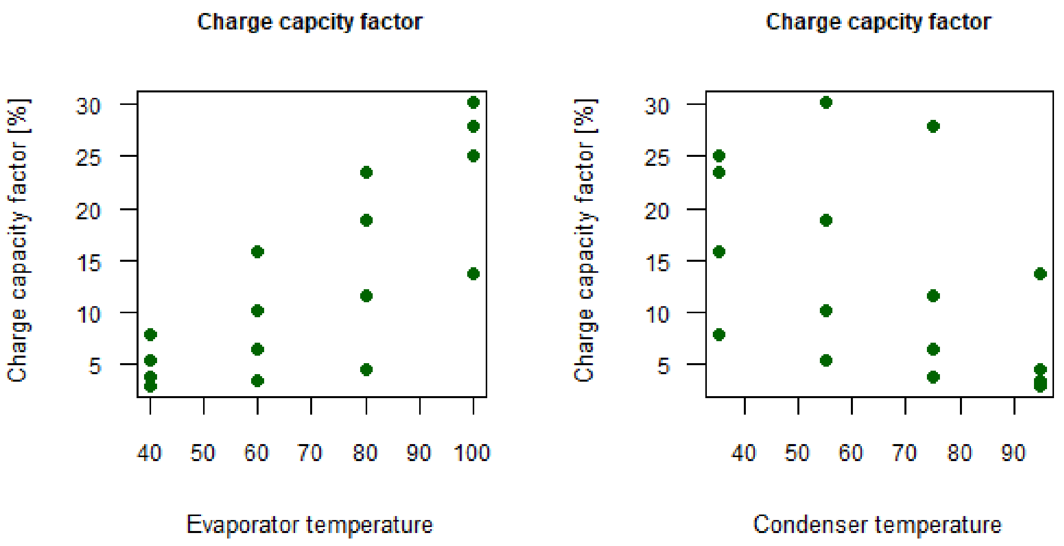

Figure 21: Charge capacity factor as a function of evaporator (left) and condenser (right) temperatures

We see that for low evaporator temperature and high condenser temperatures the capacity factor is lower. In the case of the ORC loop, we can see the variations on the capacity factor in Figure 16:

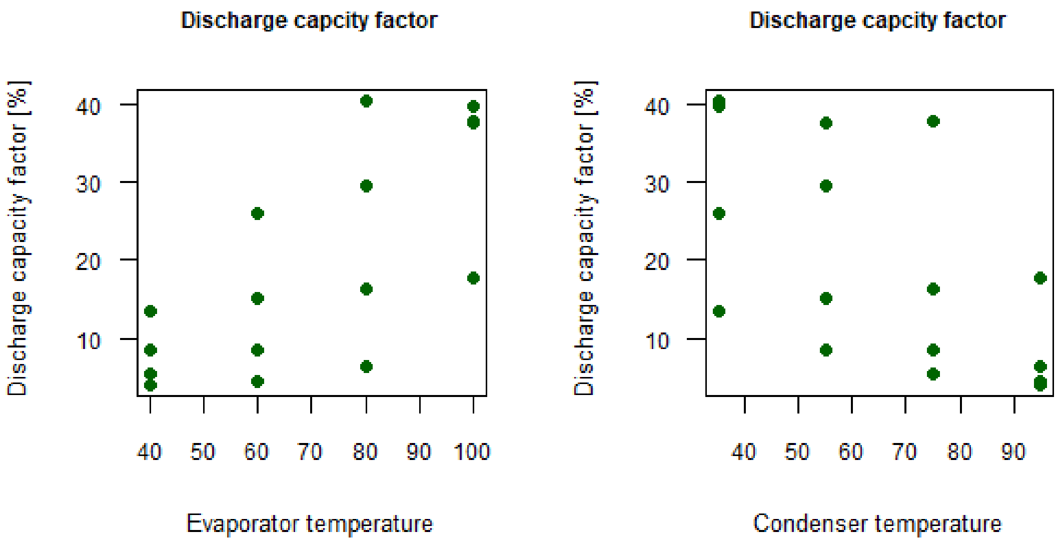

Figure 22:Discharge capacity factor as a function of evaporator (left) and condenser (right) temperatures

Again, we find that the capacity factor grows for better performing systems, corresponding to lower condenser temperature and higher evaporator temperature. This plot, together with figure 15 points that capacity factors of 70 % are achievable by a good optimisation of the control strategy.

The interpretation of this results is linked to the system model control, that is, the criteria to set the operation of the system as charging, discharging or idle; this is done by an optimiser that maximizes the operation profit of the system, considering as the running costs the price for buying and selling electricity in the most favourable of the markets available at each time of the year. The different temperature levels at the evaporator and condenser, yield a different distribution of the energy within the system into thermal energy and electricity, and also determines the overall efficiency of the CHEST, since it affects the HP COP as well as the ORC efficiency.

This has implications on the control, as can be seen by a simplified analysis of the economic balance of the system. We can make an estimate of the amount of electricity generated by storing 1 MWh of electricity; in that case, the amount of heat stored by the CHEST will be:

$$E_{th}^{stored} = (COP + 1) \quad [MWh_{th}]$$

Assuming we have the same latent ratio on both loops (HP and ORC), and disregarding thermal losses, the amount of electricity discharged from storing 1 electrical MWh would be:

$$E_{el}^{discharged} = (COP + 1) \cdot \eta_{ORC} \quad [MWh_{el}]$$

This means that the amount of electricity we are able to sell after buying 1 MWh depends on the system performance. We can translate this energetic relationship into incomes and revenues to get a threshold on the selling and buying prices; if we buy 1 MWh electric and stored, we get approximately $(COP + 1) \cdot \eta_{ORC}$ when discharging (selling) so as we need the income from selling greater than the costs for buying we have:

$$1\ MWh_{el} \cdot Price_{el}^{buy} > (COP + 1) \cdot \eta_{ORC} \cdot Price_{el}^{sold}$$

Where:

$Price_{el}^{buy}$ is the cost of the electricity purchased from the grid (stored), in €/MWh

$Price_{el}^{sold}$ is the income of the electricity sold to the electrical market (discharged), in €/MWh

The previous relation can be rearranged as:

$$\frac{Price_{el}^{buy}}{Price_{el}^{sold}} > (COP + 1) \cdot \eta_{ORC}$$

This is just an approximate expression, but still allows us to set a linear relationship between the electrical market prices and the components performance.

In the case of having a high efficiency CHEST (that is, high HP COP and ORC efficiency), the difference of market prices allowing for a profitable system operation gets reduced, when compared to smaller values of COP or efficiency. To understand the implications of this expression in the system operation and performance, we can look at Figure 15.

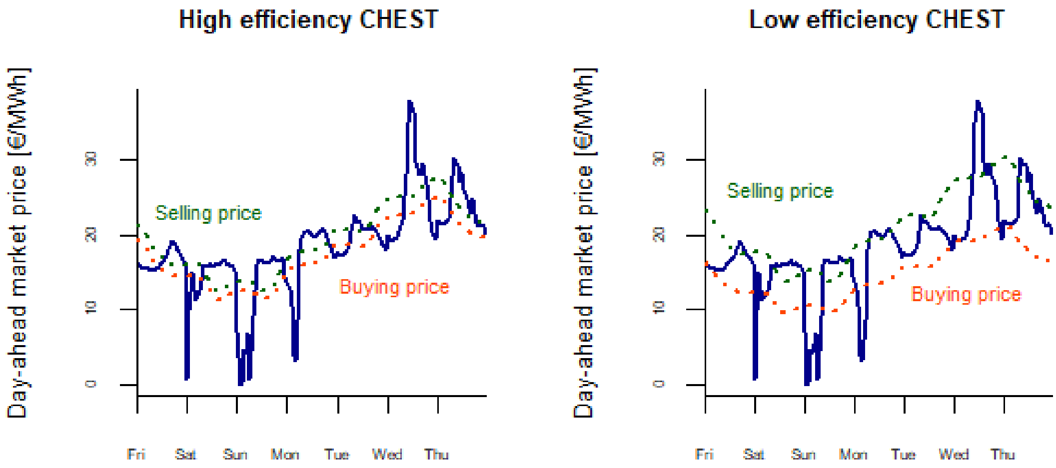

Figure 23:Comparisson of market operation strategy for different CHEST efficiencies

In the left plot of Figure 23 we represent the threshold prices for selling and buying electricity for a system with high efficiency, roughly COP=5 and ORC efficiency= 0.15. We see that for all the days within the represented week, we find many opportunities for charging (the market price goes over the green line) and discharging the storage (when the market price goes under the orange line). This means that the system will operate more time when compared to the right plot, where we represent the market prices for a scenario with approximately COP=4.2 and ORC efficiency=0.12. In other words, the system efficiency together with the shape of the electricity market prices, limit the potential for the utilisation factor of the CHEST system. From an exploitation point of view, this is a double penalisation: for a low performing system, the operation will be less efficient and, thus, the specific income per MWh stored gets reduced. Having said that, there will also be a reduction in the capacity factor due to the fact that less market opportunities will appear to get a positive operation in economic terms.

This can be seen in the two plots in the next figure, Figure 17, where we show the relationship between the P2P ratio of the simulations against the charge capacity factor (left) and discharge capacity factor (right):

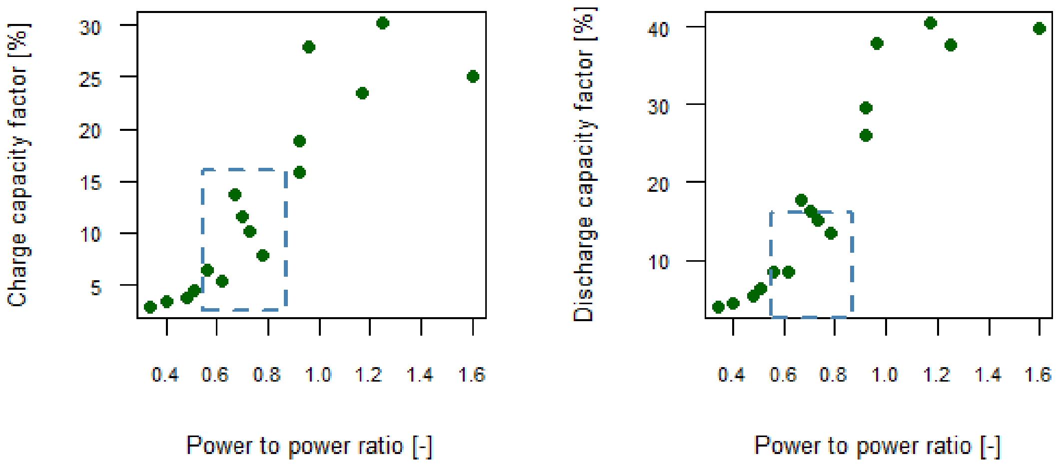

Figure 24:Simulation P2P of the scenarios as a function of charge and discharge capacity factor

It seems evident from the previous plots that the P2P ratio strongly determines the capacity factor. Both capacity factors show a similar trend: initially, for P2P ratios under 0.6 the capacity factor grows slowly but yield very low values. Then, it grows very fast up to P2P ratios of 1.0 approximately where it gets stagnant, and with increasing P2P ratios it appears to be no improvement on the capacity factor, which is around 70 % when we add the charge and discharge capacity factor, already a high value for a typical electrical market asset. Thus, it is expected that a maximum P2P ratio between 1.0-1.2 will maximize the utilization factor, and further improvements of this parameter will yield a comparatively reduced improvement in the operation profit.

The blue box in the plots at Figure 24 indicates the range of values of capacity factor and P2P ratio of the Pumped Hydro Storage (PHS) systems operating in European electricity markets. The range of P2P ratio (often called productivity in the hydroelectric sector) is taken from the national average productivity in 14 European countries, that range from 54.8 % at Norway to 86.8 % in Greece [14]. For the utilization factor, we represent data from the IEA [15], that for Europe gives values in the range from 2 % to 17 % (data for charging).

There are two considerations to point out under this comparison. The first one is that the CHEST system is able to surpass the performance of the current state of the art technology for electricity storage in the electrical grid: with appropriate heat sources, the efficiency of the CHEST system can be double the efficiency of PHS. This means that the competitiveness of the CHEST system is not limited by the system efficiency, instead, the limiting factor are the high investment costs. The second consideration is that CHEST systems with similar efficiency as PHS give utilization results similar to PHS. This seem to indicate that the present modellisation of the electricity market operation for the CHEST system is in line with the current electricity market practices for electrical storage systems.

To summarize the considerations so far, we have that the system P2P ratio has a strong impact on the utilization; besides, it is straight forward that the higher P2P ratio gives better economic results per each MWh stored, so the sum of this two factors has obvious implications on the economic return; Figure 18 shows the relationship between the operation profit and the system capacity factor:

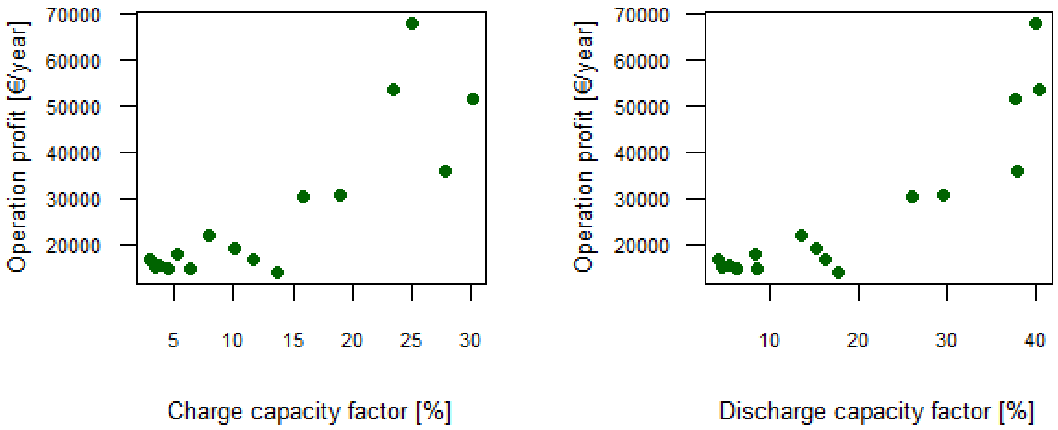

Figure 25:Simulation operation profit of the scenarios as a function of charge and discharge capacity factor

Here, the operation profit considers only incomes and revenues associated with buying and selling electricity, since in WP4 we are interested in optimising the system operation. There is a clear tendency for higher revenues with increasing capacity factors, especially for the ORC. This confirms that a frequent utilization, in a daily basis, maximises the economic balance of the system. The shape of the plots is similar to the Figure 24; in this case, we have a low operation profit for capacity factors under a value between 20 to 30 %, and after that threshold, a sudden exponential growth in the operation profit. When comparing with data on Figure 17, this threshold appears in a P2P ratio between 0.8 and 1.0.

Besides the system operation profit, we are interested in minimising the heat consumption by the system. This minimisation will increase the implementation potential of the CHEST as well as improve the economic balance, so under similar performance in terms of electricity storage we will choose those solutions with reduced heat consumption. We already described in section 2 that the situations with higher operation profit also show a bigger heat consumption, and this tendency is seen also in the simulations results of the different operation modes. This can be seen in the figure 26, where we show the relation between operation profit and heat consumption.

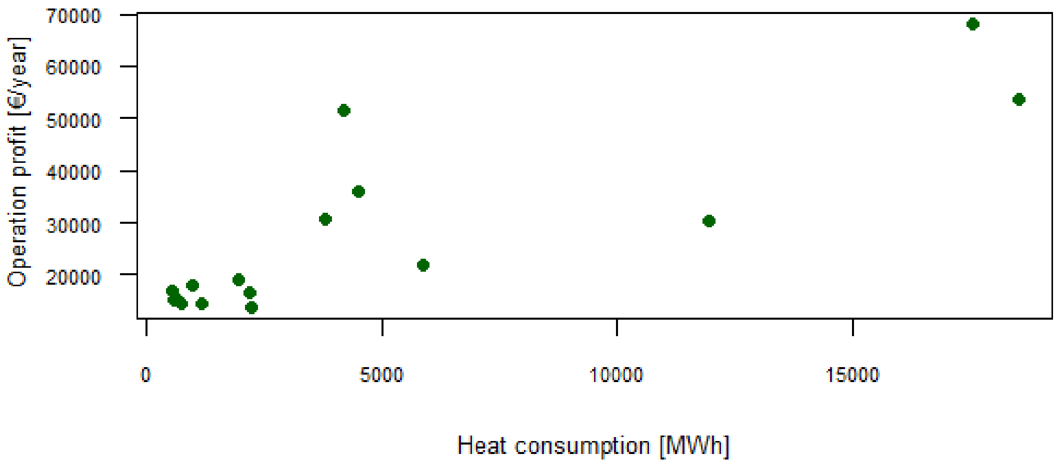

Figure 26: Operation profit vs heat consumption for the simulated operation modes

As said, there is a tendency of growing heat consumption with increased operation profit, although it is not systematic. To get a better understanding of this behaviour, we plot the heat consumption as a function of the evaporator and condenser temperatures in each simulation:

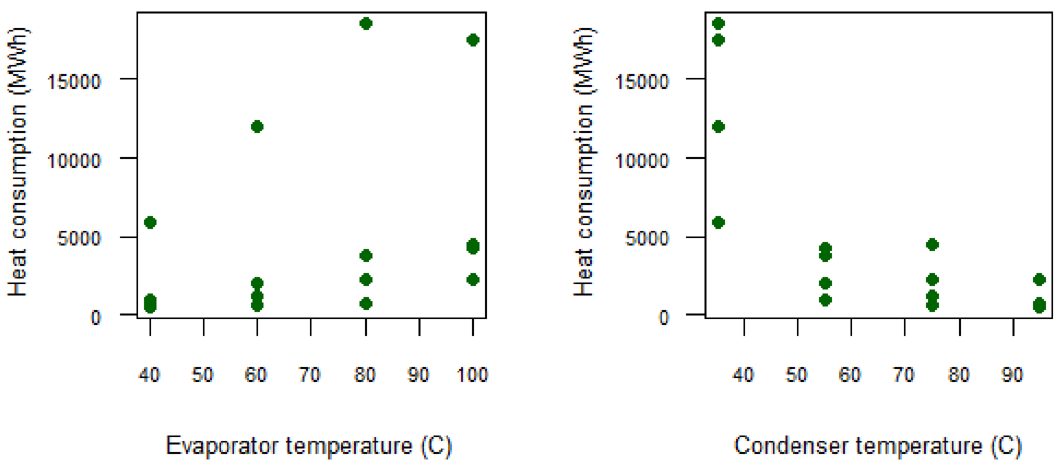

Figure 27: Plot of heat consumption as a function of evaporator temperature (left) and condenser temperature (right)

On the right frame of figure 27, we see a marked difference between the simulations at condensing temperature of 35 C and the rest of the results. This is because at such low temperatures it is not possible to reuse the condensing heat to feed the DH network at Aalborg. For the rest of the simulated scenarios, the heat demand is clearly reduced, as part of the condensing heat is recovered and reinjected into the DH. On the left side of figure 20, the dependency on the evaporator temperature is more limited than for the condenser temperature.

Since we have seen before that the capacity factor achieved by the CHEST is very different among the simulation sample, it is more clarifying to analyse the specific heat consumption.

Figure 21 shows the operation profit per unit heat consumption. As a function of the evaporator and condenser temperature:

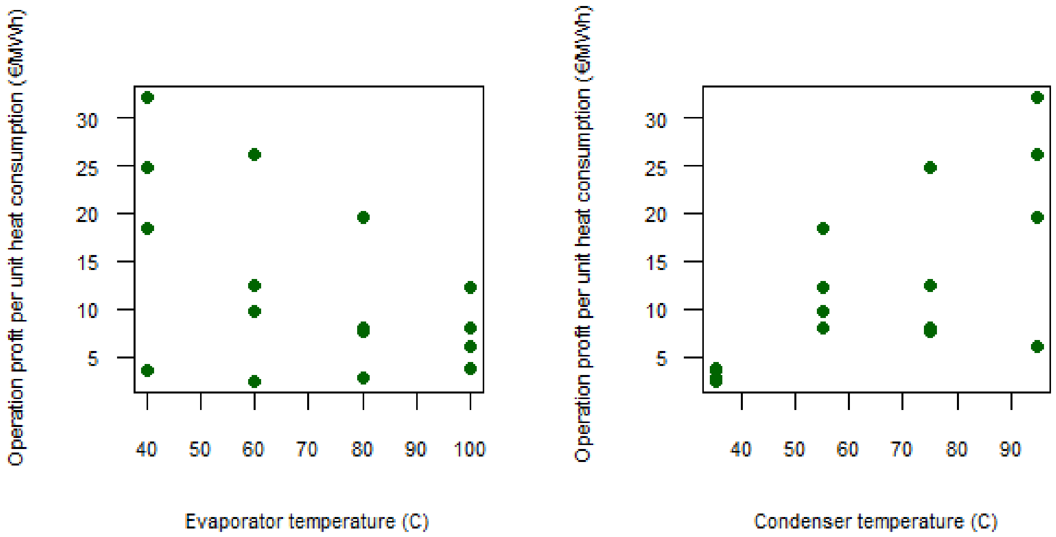

Figure 28: Operation profit per unit heat consumption as a function of evaporator and condenser temperatures

The results are a bit low, when compared with the current heat prices; as a side note, the average cost of the natural gas in EU28 for is 28.1 €/MWh according to Eurostat [16]. Although it is obvious that the CHEST system should preferably rely on some sort of residual heat, which should be purchased at lower prices, especially for lower temperature heat, it is a good reference to situate the values in figure 21. The maximum operation profit per unit heat consumed is 32 €/MWh, but most of the simulated scenarios display much smaller values, in the range of 10 to 25 €/MWh. The scenarios with condenser temperatures under the district heating operation temperature have a much worse performance, under 5 €/MWh. This is excessively low, and implies that the CHEST system has to either reuse part of the condensation heat or reduce the HP evaporator temperature to allow for low value heat sources or even ambient air energy.

5. Conclusions

Based on the selection of results presented in this deliverable, we can summarize a set of relevant conclusions for the CHEST system.

First, regarding the comparison of the system performance working with different PCM and refrigerant combinations, it is clear that the specific solution will strongly depend on the specific characteristics of each site. For the analysis in section 3, we see that the most appropriate combination for Aalborg and Ispaster case studies are different, and the reason is the available heat source and sink temperatures. Nevertheless, a set of relevant trends have been identified, for instance, the increased system performance with increasing PCM melting temperature, as well as the reduced heat requirement with increasing latent ratio of both HP and ORC loops. This can point the development of the CHEST system in the future, since those are consistent tendencies independent of the materials selection, and, as has been shown in this report, there is the potential to reduce the system size up to 40 % (thus reducing investment costs substantially) and to improve revenues up to 400 % when compared to the previously selected refrigerants. Although this puts the HP technology to its current technical limits, the development of the high temperature heat pumps has followed a fast development and it is reasonable to expect a continuous improvement and higher achievable temperatures due to the investments compromised in the field.

Another interesting conclusion regarding this materials comparison is the inverse relationship between the performance of heat services and electricity services provided by the CHEST system. It has been shown here that when the electricity services revenues increase, there is always an increase of the heat demand for the CHEST system. So, if CHEST systems has to provide electricity storage services to the grid, the heat services are hampered by the increasing heat demand of storing and generating electricity. Moreover, it has been shown that in general, the CHEST system is a net heat consumer, so it is difficult to elaborate a business model based on providing heat services, unless in a very limited extent. This is however the scope of WP6, and there the most appropriate business model will be elaborated based on these results and many other inputs from the project partners.

Regarding the operation modes of the system, it has been shown that the CHEST is able to surpass from a technical point of view the performance of the state of art technologies providing electricity storage services to the grid. Under the appropriate boundary conditions, the CHEST performance can reach electrical efficiencies up to 100 % or beyond, with comparable response time and reduced land requirements. This appears odd at first sight, but is motivated by a high heat consumption on the evaporator that is later expanded by the ORC, meaning that we are relying not only on the stored electricity, but also, on the heat absorbed at the evaporator. This, as mentioned previously, comes at the cost of increased heat consumption. However, as already identified in other deliverables; a high performance can hardly recover the investment associated with the system, so under the current electricity market prices the feasibility of the system in economic terms is not achievable. It is expected, however, that under the constant increase of the renewable electricity generators in the electricity market, prices will evolve to eventually reach the required market values to make CHEST feasible in economic terms.

The best results in economic terms have high evaporator and low condenser temperatures as a consistent tendency. This was expected due to the implications on the HP and ORC performance of this variables, but here we show that the higher revenues per thermal MW consumed are associated with high enough condensing temperatures that can be reused by an external source. Hence, in the presence of a heat consumer, the condensing temperature should be set to a value high enough to use further after expansion at the ORC. This penalises the performance, but increases the economic figures of the system. For the evaporator temperature, higher values are preferable, but the best solution to limit the heat demand would be to have very low values at the evaporator, to the level of ambient temperature. It has been shown that this reduces the capacity factor, but would improve the CHEST potential by removing the physical relation with a waste heat source. It would be interesting to explore different compression cycles for the HP that can achieve higher temperature lifts, but at the end, the real solution for a given situation will be a balance between system efficiency and thermal energy consumed.

References

[1] S. Klein and e. al., "TRNSYS 18: A Transient System Simulation Program," Solar Energy Laboratory, University of Wisconsin, Madison,USA2017.

[2] H. Jockenhöfer, W.-D. Steinmann and D. Bauer, "Detailed numerical investigation of a pumped thermal energy storage," *Energy,* no. 145, pp. 665-676, 2018.

[3] C. Arpagaus, F. Bless, M. Uhlmann, J. Schiffmann and S. Bertsch, "High Temperature Heat Pumps: Market Overview, State of the Art,Research Status, Refrigerants, and Application Potentials," in *17th International Refrigeration and Air Conditioning Conference*, Purdue, 2018.

[4] A. Crespo, M. Barreneche, M. Ibarra and W. Platzer, "Latent thermal energy storage for solar process heat applications at medium-high temperatures - A review," *Solar Energy,* no. 192, pp. 3-34, 2019.

[5] K. Du, J. Calautit, Z. Whang and H. Liu, "A review of the applications of phase change materials in cooling, heating and power generation in different temperature ranges," *Applied Energy,* no. 220, pp. 242-273, 2018.

[6] K. Reddy, V. Mudgal and T. Mallick, "Review of latent thermal energy storage for improved material stability and effective load management," *Journal of Energy Storage,* no. 15, pp. 205-227, 2018.

[7] PCM Products Ltd, "Product catalogue," [Online]. Available: http://www.pcmproducts.net/Phase_Change_Material_Products.htm. [Accessed November 2020].

[8] J. P. daCunha and P. Eames, "Thermal energy storage for low and medium temperature applications using phase change materials - A review," *Applied Energy,* pp. 227-238, 201.

[9] CHESTER D2.2, "Description of CHESTER simulation model and results," 2019.

[10] CHESTER, "D3.2: Detailed design of the high temperature heat pump laboratory prototype," 2019.

[11] A. Hassan, J. Payá and J. Corberan, "Numerical analysis of the CHEST system using different refrigerants," CHESTER internal document, 2019.

[12] L. Lindeman, "Thermodynamic analysis of a high temperature heat pump coupled with an organic rankine cycle for energy storage," Master Thesis, University of Valencia, 2018.

[13] SmartEn, "SmartEn Map: European balancing markets," 2018.

[14] C. Bott, I. Dressel and P. Bayer, "State-of-technology review of water-based closed seasonal thermal energy storage systems," *Renewable and Sustainable Energy Reviews,* vol. 113, no. 109241, 2019.

[15] I. Kougias and S. Szabo, "Pumped hydroelectric storage utilization assessment: Forerunner of renewable energy integration or Trojan horse?," *Energy,* no. 140, pp. 318-329, 2017.

[16] International Energy Agency, "Range in capacity factors over 2000-2016," [Online]. Available: https://www.iea.org/data-and-statistics/charts/range-in-capacity-factors-over-2000-2016. [Accessed 18 September 2020].

[17] Eurostat, "Gas price by type of user," [Online]. Available: https://ec.europa.eu/eurostat/databrowser/view/ten00118/default/table?lang=en. [Accessed 2020 09 18].